ERDC/CERL TR-21-6

US Army Corps of Engineers®
Engineer Research and Development Center

Automated Construction of Expeditionary Structures (ACES)

Energy Modeling

Brandy N. Diggs, Richard J. Liesen, Sameer Hamoush, Ahmed C. Megri, and Michael P. Case

February 2021

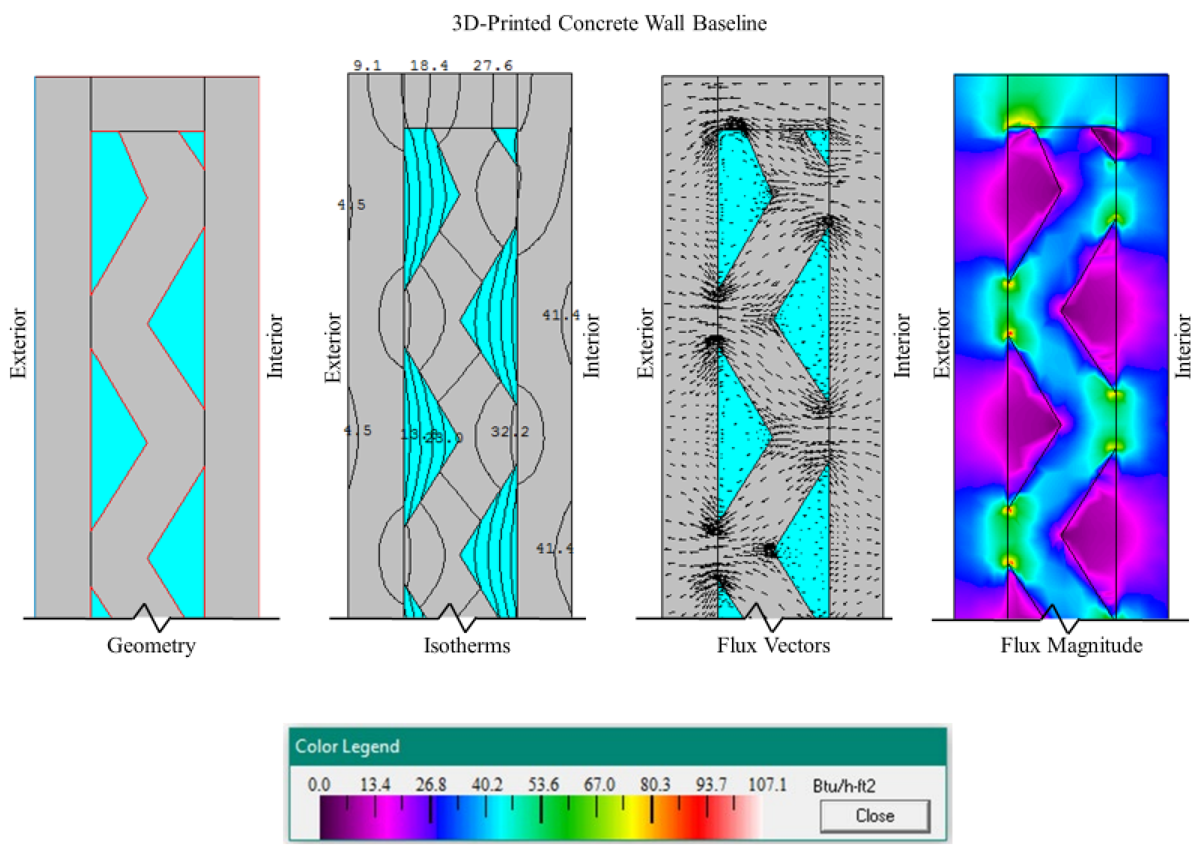

Construction Engineering Research Laboratory

ERDC/CERL TR-21-6
February 2021

Automated Construction of Expeditionary Structures (ACES)

Energy Modeling

Brandy N. Diggs, Richard J. Liesen, and Michael P. Case

U.S. Army Engineer Research and Development Center (ERDC)
Construction Engineering Research Laboratory (CERL)
2902 Newmark Dr.
Champaign, IL 61824

Sameer Hamoush and Ahmed C. Megri

North Carolina A&T State University
1601 E Market St, Greensboro, NC 27401

Final Report

Prepared for Headquarters, U.S. Army Corps of Engineers
Washington, DC 20314-1000

Under 622784T41, “Military Facilities Engineering Guidance”
622784T45, “Energy Technology Application Military Facility Guidance”
633728002, “Environmental Compliance Technology Guidance”

Abstract

The need to conduct complex operations over time results in U.S. forces remaining in deployed locations for long periods. In such cases, more sustainable facilities are required to better accommodate and protect forward deployed forces. Current efforts to develop safer, more sustainable operating facilities for contingency bases involve construction activities that redesign the types and characteristics of the structures constructed, reduce the resources required to build, and reduce resources needed to operate and maintain the completed facilities. The Automated Construction of Expeditionary Structures (ACES) project was undertaken to develop the capability to "print" custom-designed expeditionary structures on demand, in the field, using locally available materials with the minimum number of personnel. This work investigated large-scale automated "additive construction" (i.e., 3D printing with concrete) for construction applications. This document, which documents ACES energy and modeling, is one of four technical reports, each of which details a major area of the ACES research project, its research processes, and associated results, including: System Requirements, Construction, and Performance; Energy and Modeling; Materials and Testing; Architectural and Structural Analysis.

Contents

Figures and Tables

Figures

Tables

Preface

This study was conducted for the Assistant Secretary of the Army for Acquisition, Logistics, and Technology (ASAALT) under Programs: 622784T41, "Military Facilities Engineering Guidance"; 622784T45, "Energy Technology Application Military Facility Guidance"; and 633728002, "Environmental Compliance Technology Guidance"; Business Area: "Environmental Quality – Installations"; Thrust Area: "Infrastructure for Combat Operations"; Work Package: "Automated Construction of Expeditionary Structures." The technical monitor was Kurt Kinnevan, CEERD-CZT.

The work was performed by the Energy Branch, of the Facilities Division, U.S. Army Engineer Research and Development Center, Construction Engineering Research Laboratory (ERDC-CERL); by the Force Projection & Sustainment Branch, of the Research & Engineering Division, Engineer Research and Development Center, Cold Regions Research and Engineering Laboratory (ERDC-CRREL); and by the Concrete and Materials Branch, of the Engineering Systems and Materials Division, Engineer Research and Development Center, Geotechnical and Structures Laboratory (ERDC-GSL). At the time of publication, Ms. Giselle Rodriguez was Chief of the Energy Branch; Ms. Michelle Hanson was Chief of the Facilities Division; and Mr. Kurt Kinnevan was the Technical Director for Installations. The Deputy Director of ERDC-CERL was Ms. Michelle Hanson and the Acting Director was Dr. Kirankumar V. Topudurti. Dr. Toyoaki Nogami, was Chief of the Force Projection & Sustainment Branch, and Dr. Loren Wehmeyer was Chief of the Research & Engineering Division. The Deputy Director of ERDC-CRREL was Mr. David B. Ringelberg, and the Director was Dr. Joseph L. Corriveau. Mr. Christopher M. Moore was Chief of the Concrete and Materials Branch; Dr. Gordon W. McMahon was Chief of the Engineering Systems and Materials Division. The Deputy Director of ERDC-GSL was Dr. William P. Grogan, and the Director was Mr. Bartley P. Durst.

COL Teresa A. Schlosser was Commander of ERDC, and Dr. David W. Pittman was the Director.

1 Introduction

1.1 Background

After the “Cold War,” the need for forward positioned Continental United States (CONUS) type installation facilities disappeared and a new dynamic evolved. The Armed Forces needed to become expeditionary in nature. U.S. Forces needed the capability to deploy to any location and establish the means to conduct joint military operations, to successfully conduct those operations, and then to retrograde back to their “home station.” The U.S. Army is currently in the midst of a paradigm shift characterized by the ability to project its military power abroad from a CONUS base in an expeditionary manner. The changes from how Cold War operations were conducted and how future missions will be conducted are significant. However, there is one common thread between them, the need to be able to “encamp” a military unit at any location on the earth with requisite operational support capabilities (Department of Army 2008).

Since 1989, the United States has engaged in numerous military operations across the Middle East, Central Asia, Africa, Europe, South America, the Pacific Basin, and the Caribbean. For the foreseeable future, U.S. forces will likely continue to operate in a global environment of persistent conflict, characterized by protracted confrontation among numerous actors who use violence to achieve political and ideological desired end states. Military operations will involve the commitment of U.S. forces to operations in environments characterized by complex rural and urban terrain, lack of front lines, insecure flanks, dismounted combat, and constantly-fluctuating situations. Many operations will take place over large areas in austere and demanding environments, making the safety of those lines of communications and force protection for the associated logistics units an operational imperative for the commander.

To contend with the uncertainty and the many security challenges of the expeditionary condition, the U.S. military will require bases and stations within and beyond Western Europe and Northeast Asia, and temporary access arrangements for the long-distance deployment of U.S. forces (Obama 2010). Protecting the United States also requires the integration of military capabilities with other government and law enforcement agencies to manage the consequences of an attack or natural disaster (Mullen 2011).

As the Army transforms to fill these needs, the power projection platform from which the Army operates will also need to transform itself in a number of ways:

- Deployed forces will need to evolve into more self-sufficient organizations.
- Base camp footprints will need to shrink correspondingly.
- The resources needed to construct and maintain bases will need to migrate from imported materials to ubiquitous, locally recognized and used materials.
- Construction requirements for materials, personnel, and time to construct will need to decrease.
- Constructed structures will need to be more modular, scalable, adaptable, supportable by local infrastructure, and more energy efficient and survivable.

In many instances, the need to conduct complex operations over time results in U.S. forces remaining in these locations far longer than initially anticipated. Consequently, more sustainable facilities are required to better accommodate and protect the many forward deployed forces who remain for extended periods. The changing threat posture in these locations also introduces the requirement that facilities be designed to include improved force protection measures. These evolving facility needs and requirements across basecamp functions dramatically increases the demand for resources. Basecamp commanders and mayors frequently have to make difficult decisions on how to best prioritize efforts using the limited resources available in the harsh and austere environments of the deployed locations.

The U.S. Army conducted a Capabilities Based Assessment (CBA) on Base Camps from 2009 to 2011 and presented the results to the other Services at a conference in May 2011. The CBA identified 195 gaps and analyzed 120 for solutions. At the conclusion of the conference, the representatives from the U.S. Air Force, U.S. Navy, and U.S. Marine Corps endorsed the CBA and its findings as joint capability requirements.

The key operational outcome of the CBA effort on contingency bases was to provide the Joint Forces, operating in a Joint, Interagency, Intergovernmental, and Multinational (JIIM) environment at all levels, with contingency locations that can enable force projection and application (TRADOC 2009). To provide this physical location for force application, the Joint Force will require capabilities to construct and operate contingency locations in the most effective and efficient manner. Likewise, these capabilities must support the operational mission in the most effective, efficient, and sustainable manner. They also must be approached in a manner that capitalizes on their interdependence in order to provide the combatant commander the following force multiplying effects:

- Reduced threat opportunities for attacks due to smaller logistics footprints while still supporting the same level of operational capabilities and readiness.
- Increased flexibility in base operations support through improved standardized designs that are modular, scalable, adaptable, and interoperable between the Services.
- Decreased construction and deconstruction requirements (time, material, equipment, manpower).
- Improved operations management (power, water, and waste) that reduce military, civilian, or contractor oversight and support.
- Improved design of major utility backbones that support operational agility because they are designed for maximum occupancy and duration or are extensible as plans change.
- Improved safety and occupational health elements for all aspects of contingency location life cycle to prevent and minimize casualties, damage to property, and minimize risks of acute or chronic illness or disabilities.
- Improved security and protection (including protection from chemical, biological, radiological, and nuclear [CBRN] agents) that reduces diversion of manpower and other resources from operational missions.

Recent contingency operations have shown that vulnerabilities to U.S. forces occur at our bases both “inside the wire” and during logistics supply activities “outside the wire.” To mitigate these vulnerabilities, efforts are underway to develop safer and more sustainable operating conditions for contingency bases, as evidenced by the CBAs completed by the U.S. Army Training and Doctrine Command (TRADOC) and other service organizations. Key elements of these efforts involve construction activities, more specifically: (1) the associated resources (material, personnel, and equipment) to build, (2) the types and characteristics of the structures constructed, and (3) the resources necessary to operate and maintain the facilities once construction is complete.

Construction actions require significant resources during contingency operations in the form of materials, equipment, personnel for construction, equipment, and personnel to transport and manage logistics; and facilities, equipment, and personnel to provide security.

The current construction process is labor intensive. Many of the processes common in the construction industry are similar in type and complexity to those in a number of manufacturing industries, but where the manufacturing sector has been transformed with the use of robotics and automated systems, the construction industry has not. Some technologies used in manufacturing offer viable options for many types of construction, even when they have high weight and large volume requirements.

Additive manufacturing ("3D-Printing") is the industry method for creating parts from computer designs through a layered deposition process. Additive construction is a fabrication technology that uses computer control to exploit the surface-forming capability of troweling to create smooth and accurate planar and freeform surfaces out of extruded materials at a construction scale. This research intended to develop and evaluate the capability to perform construction using an automated, additive process using locally available materials.

At the beginning of the ACES program, there were no funded research and development programs that would have provided an additive construction capability in a form that the U.S. Army could use within the next 10 years. Without the investment by the Army and the National Aeronautics and Space Administration (NASA), a deployable automated construction capability would have been unlikely to become available for 15 to 20 years, as initial efforts employed massive fixed-plant component-based approaches. With the creation of a Cooperative Research and Development Agreement (CRADA) with Caterpillar, Inc., ERDC and NASA occupied a unique, first-to-market niche in development of a mobile and deployable automated construction capability. Appendix A to this report provides details of the overall ACES project management.

The requirement for this research was staffed through the U.S. Army Maneuver Support Center of Excellence (MSCoE) using a formal review process, resulting in their full endorsement. In addition, the product manager for Combat Engineer and Material Handling Systems (PdM CE/MHS) has been engaged and has concurred that a successful research effort would be appropriate to transition to a configuration such as an Engineer Mission Module mounted on a flatrack that can be hauled by the Army's Palletized

Load System (PLS) vehicle. The Army Facilities Component System (AFCS) B-Hut was used as the baseline for footprint, envelope volume, construction requirements, and sustainment requirements.

This research resulted in a system that requires fewer personnel and less material resources for construction, security, logistics support, and operations. As the construction process becomes automated, fewer personnel will be required to build the structures and to maintain security and sustainment during and after construction. Likewise, the use of local materials for the automated process will ensure that less material will need to be shipped into the area of operations; thus, fewer personnel will be needed to provide transportation and security for these materials, and to manage the construction materials during transit and storage on site.

Automated (additive) construction of structures also improves energy efficiencies over current designs, increases durability, and provides more adaptability while at the same time requiring less resources and fewer personnel to sustain. The use of local materials as the primary source for construction material will also be greatly reduce the availability and time-to-use of the material. Figure 1 summarizes the advantages of ACES over convention construction.

Other benefits of using local materials include that fact that: (1) the structures can be designed to match existing architecture appearances and aesthetic values, (2) the structures can be built in a way that may be more acceptable for subsequent use by the host population, (3) the structures' uses are understood by the local population, and (4) maintenance and repair materials are readily available. In addition, robotic construction would permit automated application of camouflage, concealment, and deception strategies to structures as they are constructed.

Figure 1. Conventional construction vs. ACES construction.

Conventional vs. ACES

Specifications	Conventional	ACES
Construction Time	4-5 days per structure	<3 days per structure
Soldier/Contractor	8 personnel per structure	3 personnel per structure
Materials Shipped	Approx. 5 tons	Approx. <2.5 tons
Construction Waste	Approx. 1 tons	Approx. Minimal
Improve Energy Efficiency	R-2 or less	R-15 to R-30

Other objectives for ACES:

- Understanding how to use readily-available onsite materials (i.e. cement, concrete)
- Understanding performance characteristics of printed structures
- Explores ability to print different types of structures.

The Automated Construction of Expeditionary Structures (ACES) project was undertaken to develop the capability to "print" custom-designed expeditionary structures on demand, in the field, using locally available materials with the minimum number of personnel. The 3-year ACES research project is documented in four separate technical reports, each of which details a major area of research processes and associated results, including:

- System Requirements, Construction, and Performance
- Energy and Modeling
- Materials and Testing
- Architectural and Structural Analysis.

ACES research has successfully developed a system that incorporates all the key elements for safer, more sustainable contingency base facilities: (1) a capability to rapidly construct structures using less and fewer resources (material, personnel, energy, etc.), (2) the capacity to provide improved force protection measures, and (3) a requirement for less resources to operate and maintain the completed facilities. Once fully implemented, this system will help basecamp commanders and mayors resolve work priorities by reducing the demand on limited resources available in severe deployed environments. ACES will enhance power projection capabilities by improving the effectiveness, efficiency, and sustainability of U.S. forces and their basecamps.

1.2 Objective

The overall objective of this research program was to develop a technology that has the capability to construct ("print") custom-designed expeditionary structures on demand, in the field, using locally available materials, with a minimum number of personnel.

The intent was to develop a construction capability that will reduce construction time, personnel (construction, operations and maintenance, and sustainment/logistics), and materiel necessary for construction. The research sought to use existing military transportation platforms on which to mount the technology. The AFCS B-Hut will be used as the baseline for footprint, envelope volume, construction requirements, and sustainment requirements.

Specific metrics for the objectives of this effort include the need to:

- reduce construction time from 4 to 5 days to 1 day per structure
- reduce Soldier/Contractor requirements for construction from eight personnel to three personnel per structure
- reduce logistics impacts will be associated with materials shipped, personnel, and resources to sustain the structures and personnel
- decrease material shipped from out of theater from 5 tons to less than 2.5 tons
- improve energy performance of the envelope from less than R1 to greater than R15
- reduce sustainment (logistics) and operations/maintenance personnel
- reduce construction waste from 1 ton to less than 500 lbs.
- improve security during construction
- improve local population acceptance by mimicking local construction.

1.3 Approach

1.3.1 Formulation of the team

This program brought together expertise from within ERDC, collaboration with NASA's Marshall Space Flight Center (MSFC) and Kennedy Space

Center (KSC), and the academic expertise from the University of Southern California (USC) to conduct highly focused research designed to prototype an automated construction system that can fabricate a ~500 sq ft structure in less than 24 hrs. The major areas / teams were:

- Materials Formulation and Testing Team
- Hardware and Controls (Building) Team
- Architecture / Design Team
- Integrated Systems Performance Testing Team
- Energy Performance (Modeling) Team
- Structural Analysis Performance (Modeling) and Test Team
- Overall Schedule Team
- NASA Support Team.

1.3.2 Early design efforts

The overarching objectives of this part of the project were accomplished, first by investigating concrete mixture designs and admixtures to adapt locally available cementitious materials to required rheology, curing time, and strength for use in an additive delivery process.

To assist in analysis of structure characteristics, the effort included the development of physics-based models and simulations to analyze various designs for structural strength, energy efficiency, logistics savings, and labor requirements, the results of which are to be packaged for future trade space visualization that could be employed by the Engineering Resilient Systems (ERS) work effort.

One of the critical efforts to meet these objectives will be the development of a sensor-based end-effector and material flow control system capable of producing required positional accuracy and stability to enable the mounting of lightweight deposition equipment on existing military equipment. This is critical not only because it enables the delivery of the construction material in a controlled manner, but also because it reduces the number of personnel necessary to support the construction process.

Finally, to empirically prove that the results of the objective have been met, a prototype system will be developed that is capable of constructing a B-Hut equivalent structure (~500 sq ft) in 24 hours or less, including custom-designed structural beams, trusses, and vaults. These structures will then be evaluated for energy efficiency and durability. A life cycle impact analysis will be developed based on the prototype operation, on the results of empirical analysis, and on an analysis of modeling and simulation.

1.3.3 Equipment use

This report focuses on the efforts of the Energy Team, which performed the following major tasks:

1. Identified the software that produces output in best agreement with the experimental results based on the tests performed on a B-Hut at the Champaign, IL test site.
2. Predicted the change in energy consumption for different climatic scenarios (i.e., climate zones, described in detail in the following section) using the two common construction materials (wood and concrete masonry unit [CMU]).
3. Characterized the building behavior of B-Huts to determine the most significant parameters that affect energy consumption, with the ultimate goal of helping design a 3D concrete-printed B-Hut.

1.4 Scope

The scope of the ACES project was to deliver a system capable of constructing a military contingency basecamp structure (16x32 ft) within 24 hours using *locally available materials* while the scope of the companion NASA project was to deliver a system capable of building a structure using *planet resources*.

1.5 Mode of technology transfer

The results of this work will be used to develop and field the third prototype, ACES 3, which will be a full-scale mobile printer with the ability to print a 16x32x8-ft B-Hut.

2 Energy Modeling of Typical B-Hut Construction

2.1 Introduction

One of the easiest and quickest structures the military can build for administrative, operations, and living facilities is the barracks hut ("B-Hut"), which has commonly been constructed of wood (plywood) and CMU materials. The military is currently in the process of improving the construction of B-Huts for use in training and theater environments, specifically by using advanced technologies to create more sustainable structures and to reduce fuel usage.

A key aspect of constructing a more sustainable and efficient B-Hut is to characterize B-Hut energy consumption and moisture control using parametric studies, and to compare the results obtained from modeling the structure as built with alternative materials. One of the main objectives in the design of a 3-D concrete-printed model is to characterize the building's behavior and to determine the most significant parameters that affect the energy consumption. A second objective is to construct a baseline B-Hut model that can be used to predict the changes in the building performance. Once these goals are met, it will be possible to manipulate the B-Hut to enhance building performances before, during, and after construction.

2.2 Goals

The goals of this work were to:

1. Predict the change in energy consumption for different climatic scenarios (i.e., climate zones, described in detail in the following section) using the two common construction materials (wood and CMU).
2. Characterize the building behavior of B-Huts and determine the most significant parameters that affect energy consumption, with the ultimate goal of helping design a 3D concrete-printed B-Hut.

2.3 Development

As the military prepares to upgrade the B-Hut, analysis of the plywood (base case) and CMU (baseline) is used to synopsize how the 3D-Printed B-Hut would perform under similar circumstances. The construction basics for both the plywood and CMU B-Huts are:

- Dimensions: 16x32-ft with 2-ft overhang on all sides.
- Area: 512 ft^2, Volume 5200 ft^3.
- Occupancy: six to eight occupants (10-15 occupants were later tested) The occupancy of the B-Hut varies from location to location. In the WUFI® simulator, a maximum of 10 occupants were used to account for the rate at which the wall layers and HVAC system could accommodate the extra moisture generated by the breathing exhalation of the increased occupancy. According to Tenwolde and Pilon (2007), the amount of respiration influences the humidity inside a dwelling. Their calculations suggest that an individual at rest will expel about 0.2 lb/h/person of water vapor in a living space maintained at 70 °F. The simulation used 10 people, accounting for 2.0 lb/h extra vapor from exhalation (0.2 lb/h per person). Later tests included an increase in occupancy to define the moisture differences associated with increased numbers of personnel.
- No windows, front/back door.
- Initial condition of wall components: temperature, 68 °F, relative humidity, 50%.
- Inside conditions: Indoor temperature 72-75 °F for heating and 70-72 °F for cooling.
- Insulation used is 1-in. polyurethane with a thermal resistance of R-6 for the roof and above grade walls (when applicable).
- HVAC: Packaged Single Zone Air-Conditioning System (PTAC). The air-conditioning in the B-Hut is provided by a split system air-conditioning system. These systems can accommodate up to 1200 ft^2 and some models provide high Seasonal Energy Efficiency Ratio (SEER) ratings. The system used in the B-Huts is also installed by the Soldiers. The input used in the WUFI® simulator software defaults to 72 °F heating and 75 °F cooling, with 2 °F of float, with a 50% relative humidity. It is hard to determine if these temperatures can be maintained in the field. Typical thermal comfort is described by the American Society of Heating, Refrigerating, and Air-Conditioning Engineers (ASHRAE) standards recommendations for each climate (de Dear et al. 2002).
- Simulated over a 3-year time period (2013-2015).

2.4 Climate zones

The U.S. Department of Energy (DOE) identifies eight climate zones (Figure 2). ASHRAE and the International Energy Conservation Code (IECC) joined together to formulate the mapping for the climate zones in North America. Before 2004, no set climate zone map was available. ASHRAE focused on the entire country while the IECC focused on the state counties. Climate and weather have direct impacts on the energy use of commercial and residential structure. For a more energy efficient structure, the building codes require the appropriate R-value (a measure of thermal resistance) for the climate zone. Climate Zones 3 and 4 have three sub-sections, while 1, 2, 5, and 6 have two sub-sections. Climate Zones 7 and 8 only have one section. Table 1 lists the climate zones by their hygrothermal properties.

Figure 2. Detailed climate zone map.

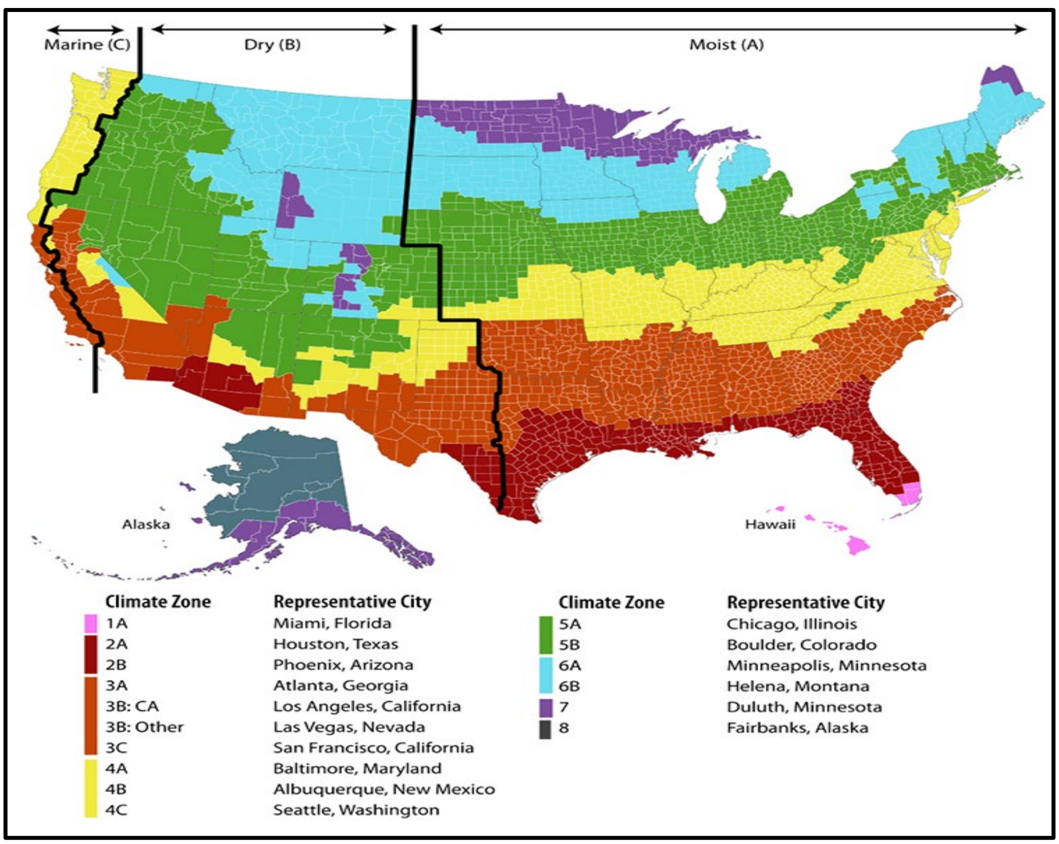

Table 1. Climate zone by hygrothermal properties.

Climate Zone	Climate Type	Climate Zone	Climate Type	Climate Zone	Climate Type
1a	Very Hot-Humid	3c	Warm-Marine	5b	Cool-Dry
2a	Hot-Humid	4a	Mixed-Humid	6a	Cold-Humid
2b	Hot-Dry	4b	Mixed-Dry	6b	Cold-Dry
3a	Warm-Humid	4c	Mixed-Marine	7a	Very Cold
3b	Warm-Dry	5a	Cool-Humid	8a	Subarctic

2.5 Energy performance

Using parametric studies to help design a B-Hut that conserves energy is key to developing a fieldable structure that is sustainable and efficient (Figure 3). This work performed a parametric study using EnergyPlus,* a whole building energy simulation program that helps analyze a variety of building materials in a single analysis. The goal was to predict the change in energy consumption for different climatic scenarios using different construction materials. By considering heat transfer phenomena such as convection, conduction, and radiation (and where they occur) in the plywood and CMU B-Huts, the data results (which vary between climate zones) may be used to form meaningful comparisons between the two materials. Tests reported here were performed using the weather data from Champaign, IL.

Figure 3. Managing energy consumption.

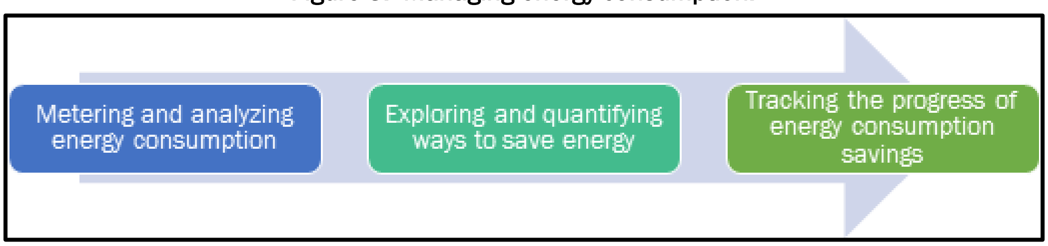

2.5.1 Data entry

Data were gathered using these steps:

1. A B-Hut model was built within the energy simulation program "EnergyPlus" using ERDC-provided specifications.
2. Various energy simulations were done for various climate zones.
3. Data were recorded in Excel workbook format.

* EnergyPlus is open-source software funded by the U.S. Department of Energy (DOE), and is freely available to the public through URL: https://energyplus.net/downloads

2.5.1.1 First simulation test – Baseline

The first simulation run demonstrated the B-Hut in operation under basic conditions, i.e., without any changes. This formed the baseline of the study for both cases, wood and CMU (Table 2). Forming the baseline gives the starting the point for the data and the relationship between the starting point and the changes that occur.

Table 2. Basic baseline information for EnergyPlus.

Type	General Conditions	Building Envelope	Air Change Per Hour (ACH)	Building Interior	Exterior Door	Non-HVAC End Uses	Hours Occupied
Plywood	No heat/cool, multifamily low-rise with exterior exits, electric/gas load rate	Roof: Standard wood frame with exterior steel, uncolored, wood plywood. Walls: Wood framed plywood 2x6, no interior insulation, over crawl space and no exterior insulation	0.038 cfm exterior wall area	Interior drywall finish, no insulation board	2 - 6.7 x 3.0-ft wood solid core flush 1⅜-in. doors one on both ends	Exterior lighting, misc. equipment interior lighting, DHW	5 pm - 7 am
Construction	No heat/cool, multifamily low-rise with exterior exits, electric/gas load rate	Roof: Standard wood frame with exterior steel, uncolored. Walls: 12-in. CMU, no exterior finish, no exterior insulation, earth contact no interior insulation	0.038 cfm exterior wall area	Interior drywall finish, no insulation board	2 - 6.7 x 3.0-ft wood solid core flush 1⅜-in. doors one on both ends	Exterior lighting, misc. equipment interior lighting, DHW	5 pm - 7 am

2.5.1.2 Task 1: Perform sensitivity analysis using different candidate HVAC systems for B-Huts by climate zone

With the baseline in place, the simulation ran the following HVAC systems for data output:

- DX Coil with Electric Resistance with Package Single Zone DX with Electric Reheat
- DX Coil with Electric Resistance with Split System Single Zone DX with Electric Reheat
- DX Coil with Furnace Heat Package Single Zone DX Furnace
- DX Coil with Furnace Heat Split System Single Zone with DX Furnace
- DX Coil with DX Coils (Heat Pump), Package Single Zone with Heat Pump
- DX Coil with DX Coils (Heat Pump), Split System Single Zone with Heat Pump.

The initial results indicated that the insulated CMUs performed better (i.e., consumed less kWh of electricity) than the non-insulated CMU. Also, comparisons of all the HVAC systems listed above showed that the package systems for each unit type performed better than the split systems.

The final test for this task was to study both CMU and plywood construction with a variety of insulation thickness changes. The "DX Coil with Electric Resistance with Package Single Zone DX with Electric Reheat HVAC" system was used as the base HVAC system. The results are explained in the Data Results sections (pp 18, 44).

2.5.1.3 Task 2: Run the EnergyPlus models into the simulated climate zones for various ACH values

The second simulation run reflected a change in ACH due to the increase in infiltration or air tightness. In addition to ACH, polyurethane insulation of diverse thermal resistances were tested. ACH is a measure of air volume removed from or added to a space, divided by the volume of the space:

$$ACH = \frac{60 * volumetric\ flow\ (cfm)}{Vol} \tag{1}$$

where:

ACH = number of air changes per hour (volumetric flow rate of air, expressed in cfm)
Vol = space volume $L \times W \times H$, in cubic feet.

The formula to express the volume rate per hour from the ventilation rate is:

$$R_p = \frac{ACH * D * h}{60} \tag{2}$$

where:

R_p = ventilation rate per person (cfm per person, L/s per person)
ACH = air changes per hour
D = occupant density (occupants per square foot, occupants per square meter)
h = ceiling height (ft, meters).

The simulations used the following ACHs:

- Plywood construction: ACHs analyzed vary from 0 to 3.00, with a step of 0.25.

- CMU construction: ACHs analyzed vary from 0 to 1.50, with as step value of 0.25.

The results are displayed in the Data Results section (p 18).

2.5.1.4 Task 3: Run the EnergyPlus models into the simulated climate zones for various ACH values and the standard insulation material, polyurethane

The third simulation runs reflected changes in insulation along with varying ACHs. The construction of residential and commercial buildings uses several types of insulation. In steady state conditions, the thermal resistance of building components (wall, roof, or floor) depends on the temperature difference across the component, the conductivity of the materials used, and the thickness of each material layer. The U-value expresses the wall conductance, air to air, which includes wall conduction, surface convection, and radiation. Heat transfer through 1 ft^2 of a structural element when the difference between the inner and outer face temperature is 1 °F, is expressed in the form of the reciprocal of the total R-value:

$$U = \frac{1}{R} \tag{3}$$

Table 3 lists the insulation values for the roof and the above grade walls used in these simulations.

Table 3. Insulation choices.

Insulation	Material	Plywood	CMU
Roof	Polyurethane	R-6, R-9, R-12 and R-18	R-6, R-9, R-12 and R-18
Above Grade Walls	Polyurethane	R-6, R-9, R-12 and R-18	R-6, R-9, R-12 and R-18

The climatic areas that were analyzed were Urbana, IL; Atlanta, GA; and Fairbanks, AK. A range of climate zones was analyzed to investigate how the insulation would drive the cost value of energy consumption and building construction for different regions. The data under investigation, pertaining to the insulation used, were:

- Plywood construction: Roof insulation: 1-in. polyurethane; wall insulation: ¾-in. fiberboard sheathing; ground earth contact (baseline)
- Plywood construction: Roof insulation: 1-½-in. polyurethane; wall insulation: 1½-in. polyurethane; ground earth contact (R-9)
- Plywood construction: Roof insulation 2-in. polyurethane; wall insulation: 2-in. polyurethane; ground earth contact (R-12) with ACH values: 1.25, 1.50, 1.75, 2.00, and 2.2.

2.5.1.5 Task 4: Run EnergyPlus models into the simulated climate zones to determine the influence coefficients (ICs)

In addition to calculations of total energy usage and energy use intensity (EUI), the IC was also determined. IC is used to pinpoint the building element (such as the HVAC system, lighting, natural gas, door, windows, etc.) that affects the performance of the structure. The IC is a ratio of the percentage change in the output to the percentage change in the input — the higher the value, the greater the influence of that element on building performance:

$$IC = \frac{\Delta OP}{\Delta IP} \tag{4}$$

where:

ΔOP = change in output
ΔIP = change in input.

The approach to data processing is to review the outputs from the original simulation run and to compare those outputs to the data from the revised model. This information can also be used to investigate implementation of the changes and uncertain parameters. This method is used to identify key issues and make the appropriate decision for building materials and construction properties. Table 4 lists the simulation specifications.

Table 4. Simulation specifications.

	Roof Insulation	Wall Insulation	Infiltration (ACH)
Plywood	Baseline, R-5, R-10, R-15, R-20	Baseline, R-5, R-10, R-15, R-20	3, 2.5, 2, 1.5, 1, 0.5
CMU	Baseline, R-5, R-10, R-15, R-20	Baseline, R-5, R-10, R-15, R-20	3, 2.5, 2, 1.5, 1, 0.5

The output data included the total kBtu, total EUI (kBtu/sq ft/yr), U-factors, and total building intensity (units):

- Total kBtus. This is a breakdown of the total energy used by the HVAC system, lighting, fans, pumps, etc. All the energy used by a facility.
- EUI. This performance indicator provides the means to equalize the way energy is used in various types of buildings, and to evaluate ways to reduce overall energy consumption if values are excessive. The formula used to calculate EUI is:

$$EUI = \frac{Btu*1000}{Total\ Area} \text{ / yr} \tag{5}$$

- U-factor. This is the measure of the resistance to heat gain or loss through any material due to the difference between indoor and outdoor air temperatures. The U-factor or U-value is also referred to as the overall coefficient of heat transfer.
- Total Building Intensity: This is the summation of the intensity of the individual components of the structure. B-Huts have electricity only, but they could also include gas and water.

2.5.2 Data results

2.5.2.1 Task 1

The data showed, using the Champaign, IL test site, that the insulated CMUs performed better in terms of saving Watt-hours compared to the non-insulated concrete masonry unit. The results also show that between all the HVAC systems, the package systems for each unit type performed better than the split systems (Figure 4).

The results also show that, between all the HVAC systems, the package systems for each unit type performed better than did the split systems (Figure 5). Figure 6 shows ACH variances for the two constructions: R-12 for plywood and CMU.

Figure 4. Load of the building over the year, under several HVAC systems (w/insulation).

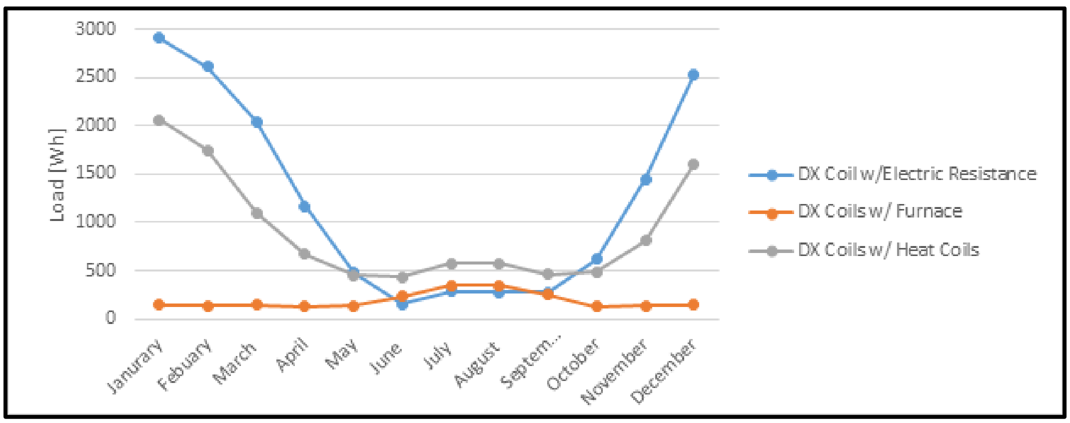

Figure 5. Load of the building over the year, under several HVAC systems (w/o insulation).

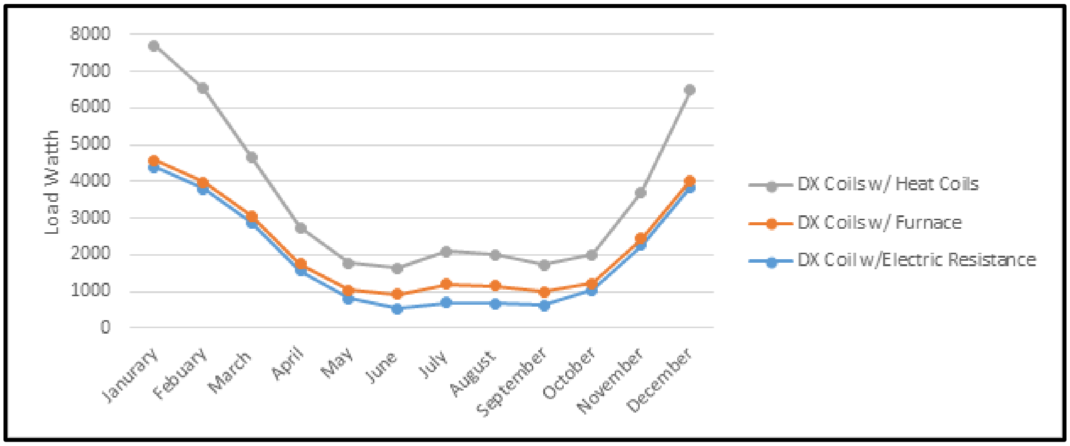

Figure 6. ACH variances for two constructions: R-12 for plywood and CMU, in Urbana, IL.

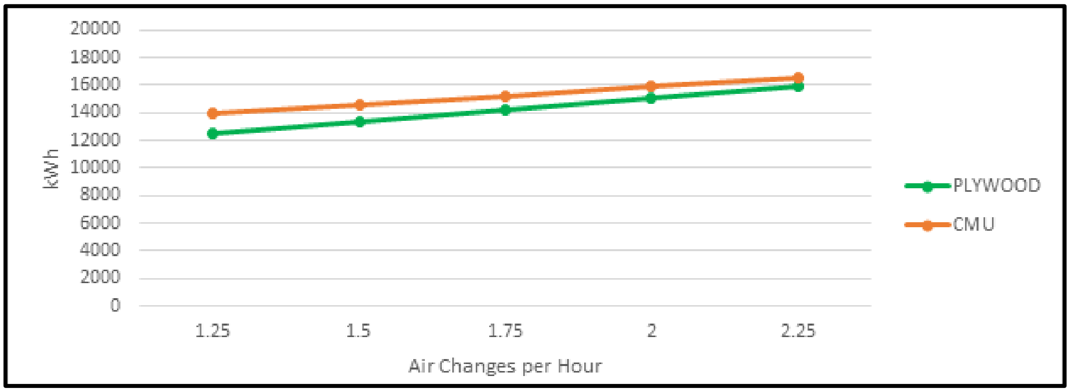

The amount of energy used (kBtu) within each case increased with the increase in air change rate. There were significant decreases in the amount of energy used when the insulation was increased. A comparison of these three very different climate zones shows that Climate Zone 3 (Figure 7) and Climate Zone 5 had only slight variations in the amount of energy used, indicating that additional insulation would not yield as significant a cost savings. However, an increase in insulation is needed in Climate Zone 8 (Figure 8) due to the nature of its climate.

The graphs in Figures 6, 7, and 8 show a linear relationship between the energy used and ACH in the plywood and CMU B-Huts. A review of the trends of the kBtus for the plywood construction might indicate that the same trend will follow with the concrete masonry units. The CMU B-Huts have lower energy loads then the plywood construction. There is an increase in energy consumption with the increase of ACH for both constructions. In EnergyPlus, the total energy output is measured in kBtus.

Figure 7. ACH variances for two constructions: R-12 for plywood and CMU, in Atlanta, GA.

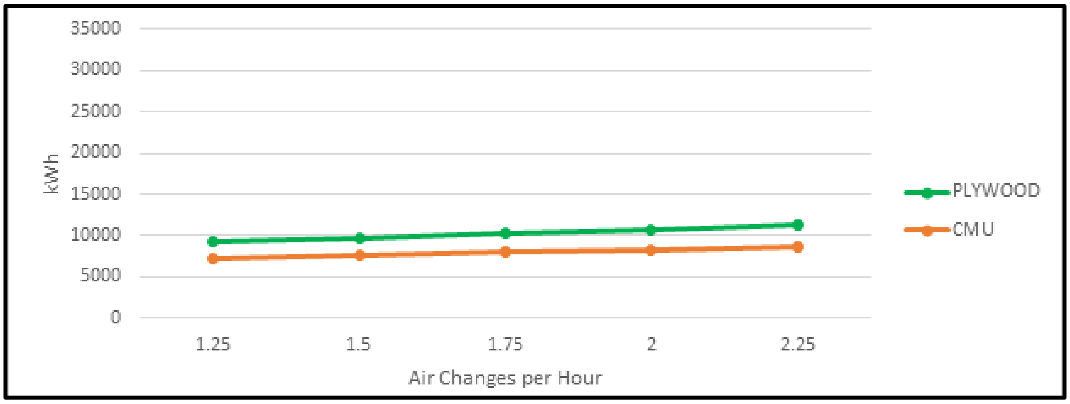

Figure 8. ACH variances for two constructions: R-12 for plywood and CMU, in Fairbanks, AK.

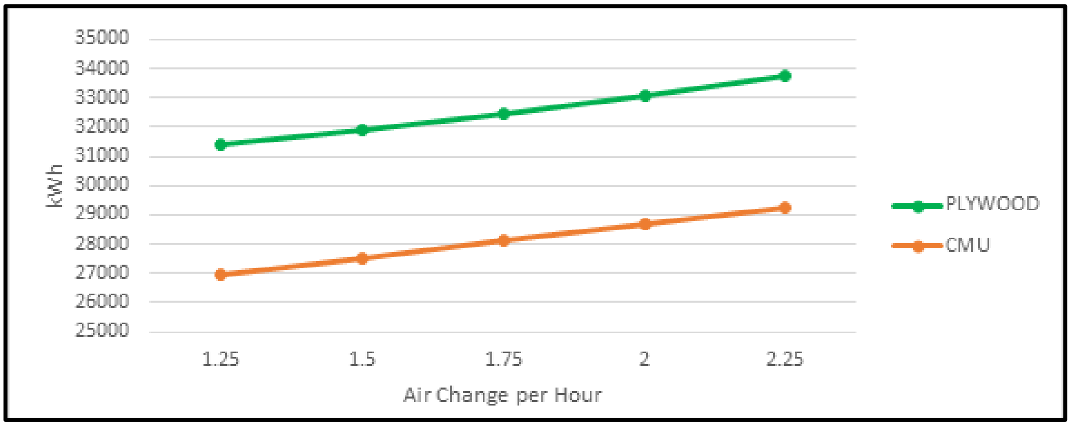

Since the results were given in kWh, they need to be converted to kBtus using this conversation factor:

$$\text{kWh} \times 3.412 = \text{kBtu} \qquad (6)$$

Then, the kBtus are divided by the total area of the space to yield the amount of kBtus per square foot:

$$\text{kBtu} / \text{total area} = \text{kBtu/sq ft} \qquad (7)$$

The calculations for the kBtu/sq ft in each insulation case were made for the area of 512 sq ft.

2.5.2.2 Task 3

For comparison, Figure 9 shows ACH variances for two constructions: R-6 for plywood and CMU.

Figure 9. ACH variances for two constructions: R-6 for plywood and CMU.

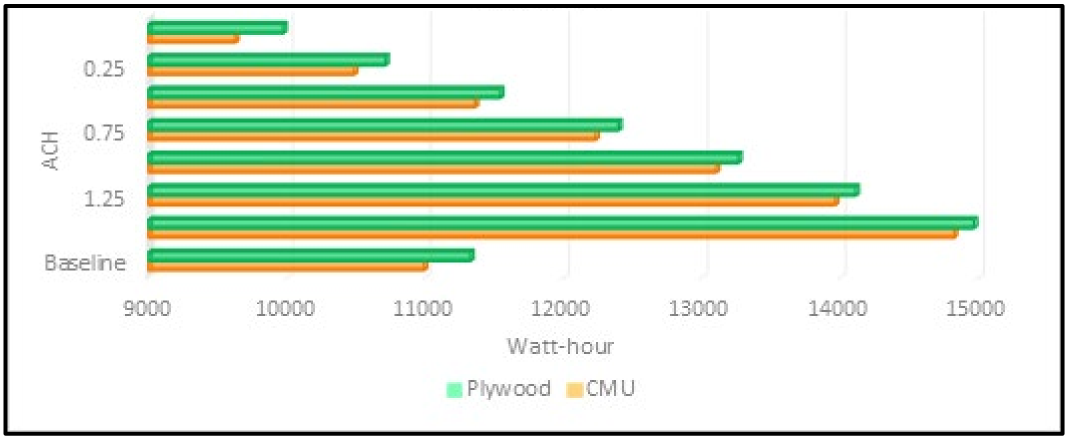

A comparison of the results for both cases of construction reveals a decrease in the energy consumption (watt-hours) as the R-values increase. The energy consumption of the concrete masonry building envelop consumed less energy (watt-hour) compared to the plywood construction. The plywood construction consisted of a ¾-in. fiberboard sheathing above the grade level (wall construction) and R-6 at the roof level. With the comparison of the R-6 value, which is standard with CMU construction, but not with the plywood construction, the CMUs performance was superior for each airflow rate of infiltration. Additionally, for each of the eight climate zones, the energy consumption of the CMUs with R-6 increased as the ACH increased.

The results show that the insulation in the barracks reduces energy consumption by 40%. In addition, the results show that tightening the building envelope will reduce the energy consumption; a reduction of 16% of the ACH decreases the load by approximately 4-8% in the case of concrete masonry units and 6-10% in the case of plywood barracks.

2.5.2.3 Task 4

In theory, as R-values increase, the amount of energy used decreases, and as infiltration increases, the amount of energy used will also increase. However, the results related to the roof insulation, wall insulation, and infiltration show that this is not always the case. The lower the IC value for each type of energy load (pumps, HVAC, lighting), the less influence it has on the total energy consumption. To effect substantial changes in the total load for the structure, the highest IC would direct the entity change to improve (e.g., lighting, HVAC system components, domestic hot water) to achieve a more sustainable building envelope.

Most heat loss is due to the area of the walls in comparison to the area of the roof. B-Huts do not have windows to compromise the insulating value of the walls. In fact, the wall area accounts for more energy loss than the roof because total wall area is greater than the total roof area, giving the wall area a high coefficient of influence, even though the roof area is more affected by solar radiation

For example, if the B-Huts are constructed by Army or local national personnel (most of whom do not have a construction background), the resulting B-Huts would be built quickly, but would most likely operate at a less than optimal energy efficiency. In such a case, an ACH infiltration value of 3.0 would be a more probable scenario than the optimal ACH of 0.5. The ACH value directly influences the amount of energy being used. For a typical B-Hut setting, this work analyzed ACH infiltrations of 2.0, 1.5, 1.0, and 0.5. Under these conditions, the plywood construction had a decreased amount of influence on the barracks. It was not until the B-Hut reaches an ACH rate of 2.5-3.0 that the concrete B-Hut began to show more favorable results than the wooden structure.

After reviewing the sensitivity analysis, the ICs can be established by taking the quantitative measures from the sensitivity model and then changing the inputs to present day attributes. The ICs helps to explain how different parameters of the building loads affect the total outcome of the building in terms of cost value. The sensitivity analysis shows where improvements need to occur, and the ICs shows how the thermal zone affects the load value. Determining these key factors advances the design of the structure as well as its energy prediction. This analysis shows how minor changes can substantially influence the total energy load of the building; it can also guide the development of monitoring processes and identify successful ways to reduce unnecessary energy waste.

The results for the three roof and wall building construction cases (Figure 10) show a negative trendline, indicating that the forecasting quantitative data would be negative with an increase in R-value insulation. The linear equation expresses the relationship between the x-value (R-value) and the y-value (energy consumption). The regression line is an accepted estimation of the relationship between the two properties, showing the range in the value.

Figure 10. The R^2 correlation between plywood, CMU1, and CMU2.

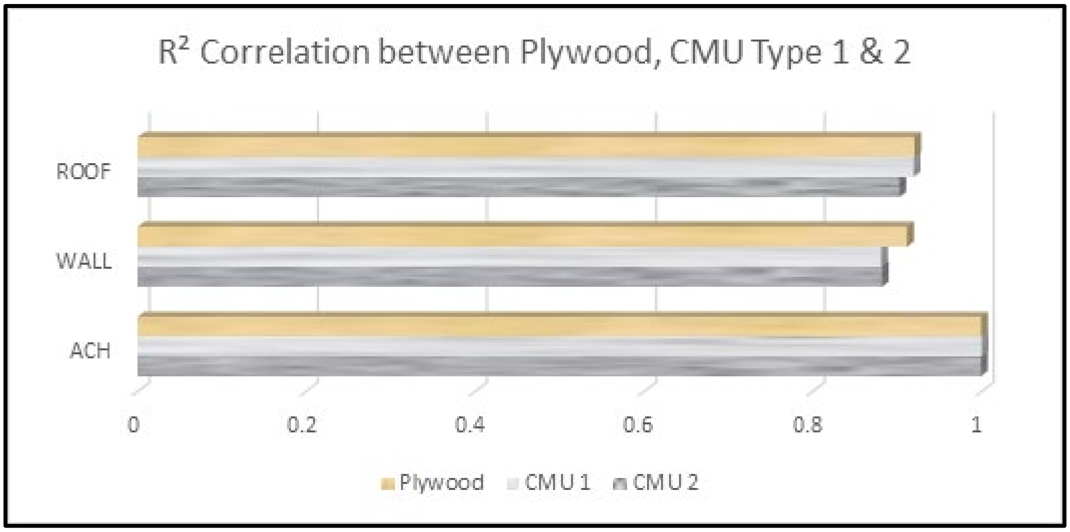

The coefficient of determination or R^2 value statistically demonstrates how closely the function fits the experimental datasets. The R^2 value ranges from 0 to 1, where a value of 1 represents an ideal fit, and 0 represents no correlation between the data and the line. In this case, air infiltration is the highest contributing factor when it comes to energy consumption.

A recognition of heat transfer phenomena, such as convection, conduction, and radiation, and where they occur in the plywood and CMU B-Huts, helps to explain the data results, and to account for the fact that these results vary in different climate zones. The experimental unoccupied B-Hut on the ERDC Champaign, IL campus was used to study real-time events such as the weather effects, indoor air quality, and thermal comfort. EnergyPlus uses typical weather data to represent the climate of a specific area for a specific time. Other factors that can affect the outcome of the simulation include building orientation and geometry, thermal characteristics of the building envelope, the HVAC systems, building use, and the occupants' behavior (i.e., their schedules).

2.5.3 Moisture control

The application of vapor barriers and retarders in appropriate places can help to control the amount of moisture diffused (Figure 11). For example, a sheet membrane of asphalt-impregnated felt or rigid insulation can provide a great deal of water control.

Figure 11. Movement of water vapor.

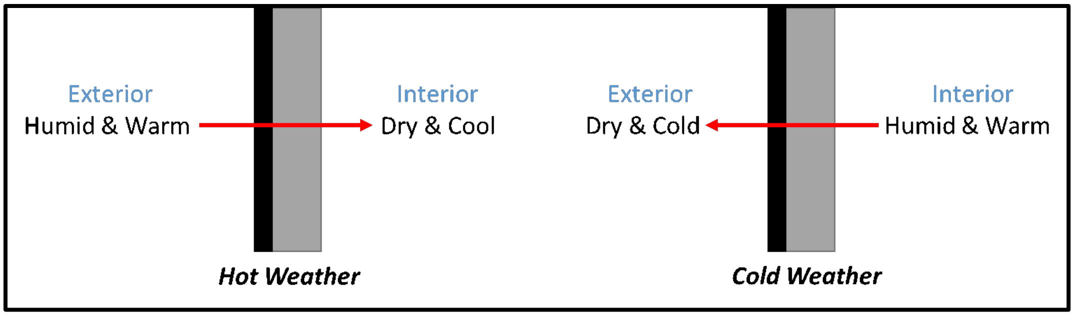

Moisture deflection via water control layers can help eliminate the threat of rot, mold, and mildew, and can easily deflect the major causes of water infiltration, such as rain and snow, but it cannot alleviate vapor diffusion or air transport through the surface. Unless properly drained, trapped moisture can collect in unaccounted for spaces and gaps, and cause unintentional, unseen damage—and more serious subsequent problems.

Lstiburek (1996) states that the building durability plays a key role. In other words, all aspects of a structure must be combined to ensure a high-quality structure in terms of durability and sustainability. Improving a building's integrity, durability, and sustainability is a cost-efficient way to extend its life cycle.

Lstiburek further describes interior climate conditions by applying moisture engineering in the hygrothermal regions. Moisture enters structures in many ways, e.g., driving rain, splash backs, windows, roof and door leaks, direct entry, surface and groundwater, freeze-thaw, built-in moisture, flooding, wet-installed materials, curing-concrete or masonry, vapor entry and movement, water movement into wall and framing, and condensation and humidity. To avoid moisture problems, proper design, construction, and quality assurance of a sustainable residential dwelling must consider the ability of the buildings' walls and roof to dry out, both inside and outside the space.

The goal of studying the infiltration of moisture into the B-Hut is to identify building materials applicable for the use with the 3D-printed B-Hut, and to analyze how those materials affect similar structures such as the CMU and (plywood B-Hut) base case. Specific desirable effects are how those materials reduce the water content stored in the building materials in various climate zones, and how they prevent further water infiltration and the occurrence of mold. Comprehensive solutions include:

- Reducing the amount of moisture stored in the building materials from the weather conditions, the operation of HVAC systems, and building occupants
- Reducing microbial growth that affects inhabitants' quality of life
- Averting the growth of spore germination.

Figure 12 illustrates mitigation strategies.

2.5.3.1 Data input

This work used the following software tools to analyze conditions in each building material layer over a given time period:

- WUFI® (a hygrothermal simulator, testing transient heat and moisture transport)*
- WUFI® Bio (a biohygrothermal model developed to assess mold growth under transient hygrothermal boundary conditions)
- WUFI® Mold Index VTT (a mathematic-empirical model predicts mold growth as a function of substrate material, temperature, and relative humidity).

The material database in the WUFI® software includes material properties such as bulk density, permeability (Table 5), layer thickness, porosity, heat capacity, thermal conductivity (moisture and thermal dependent) enthalpy, liquid transport coefficient (suction and redistribution), and the moisture storage function. This study considered the moisture storage function, permeability, and thermal conductivity as deciding factors in determining the building material that would be used at the boundaries.

Figure 12. Mitigation strategy.

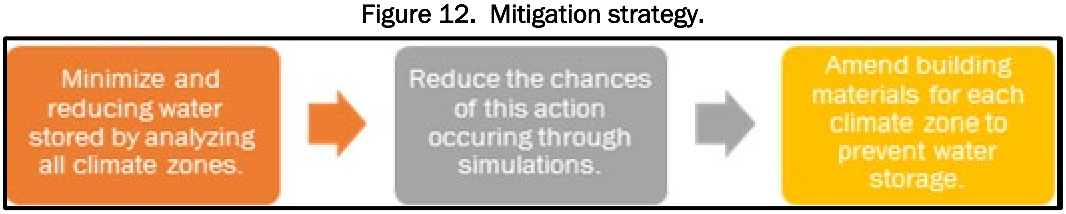

* WUFI® software is a product of the Fraunhofer Institute For Building Physics, Holzkirchen Branch, Fraunhoferstr. 10, 83626 Valley, available through: https://wufi.de/en/software/

Table 5. Permeance rating and building material examples.

Class	Permeance (U.S. perms)	Description	Building Material
I	Less than 0.1	Impermeable	Glass, Sheet Metal, Unperforated Aluminum Foil, Rubber Membrane, Polyethylene Sheet
II	0.1 to 1.0	Semi-Impermeable	30-Lb Asphalt-Coating Paper, Unfaced Expanded /Extruded Polystyrene, Plywood Bitumen-Coated Kraft Paper
III	1 to 10	Semi-Permeable	Latex Or Enamel Paint, 15-Lb Asphalt-Coated Paper, Brick, Concrete Block, Board Lumber, Gypsum Board, Fiberglass Insulation (unfaced), Cellulose Insulation
None	Over 10	Permeable	N/A

Infiltration of moisture through the wall or roof is decreased by using a proper vapor retarder in the appropriate location for maximum effectiveness. Vapor barriers and vapor retarders are often misconstrued as the same thing. While a vapor retarder is defined as having a permeance higher the 0.1 perms, but less than or equal to 1 perm. A vapor barrier has a permeance of 0.1 perms or less, which slows or stops vapor transmission. Class III vapor retarders are now allowed in various climate zones in buildings constructed to allow drying through the surfaces. This is achieved by using vented cladding to reduce condensation on the surface.

The concrete B-Hut was modeled in WUFI® using bare concrete walls. The model simulated the addition of vapor retarders of various permeance ratings on the interior and exterior surfaces to test the action of the moisture throughout the wall section. Table 6 lists the properties of the tested materials. WUFI® output data consist of moisture and heat fluxes, total water content, time, and occurrence of mold. In this case, special interest is given to in the water content of the material through the given time period. To prevent mold growth, the total water content of the given time period must be below the critical moisture content for the germination of mold spores.

Table 6. Building material properties from WUFI®.

Material Name	Bulk Density (lb/ft³)	Porosity (ft³/ft³)	Specific Heat (Btu/lb°F)	Thermal Conductance (Btu/hft°F)	Permeability (perm-in)	Typical Built-In Moisture (lb/ft³)	Layer Thickness (in)
Concrete Brick (3D Printed-B-Hut)	144.521	0.1296	0.191077	0.42352	0.705753	3.24625	9.44882
Plywood	29.3411	0.69	0.44903	0.0485343	0.119458	4.36996	0.590551
Vapor Barrier (Impermeable)	n/a	n/a	n/a	n/a	0.00219	n/a	n/a
Vapor Retarder 0.1	8.11563	0.001	0.549346	1.32892	0.00392683	n/a	0.03937
Vapor Retarder 1.0 Perms	8.11563	0.001	0.546346	1.32892	0.0392683	n/a	0.03937
Vapor Retarder 5.0 Perms	8.1156	0.001	0.54936	1.32892	0.196341	n/a	0.0.3937
Vapor Retarder 10	8.11563	0.001	0.549346	1.32892	0.392683	n/a	0.03937

2.5.3.2 Data results

It is important to model the water content through a surface because water can destroy a wall section that has not been properly dried. Vapor condensation increases total water content. If the total water content of the wall is higher than the critical water content of spores, mold growth will occur. WUFI® data detailed, by climate zone, how the placement of the vapor retarder affects the total water content of the wall. This breakdown by climate zones of a structure's susceptibility to total water content helps determine if a vapor retarder will be needed, and if it is, the type of the vapor retarder to use and where to place it.

Figures 13 to 17 help determine where the placement of the vapor retarder. Figure 13 shows the difference between B-Hut structures in five climate zones that have no vapor retarder. Figures 14 and 15 show how adding a vapor retarder on the exterior and interior surfaces affect the ability to dry out. Since concrete is classified as a Class III vapor retarder, using a retarder higher the 10 perms would not be recommended. Isolating the results by each climate zone, also narrows down where to place the vapor retarder and what permeance to use.

Figure 16 shows that adding exterior vapor retarders of 0.1, 1.0, 5.0, and 10 perms yield results similar to those of B-Huts with no vapor retarder. When adding an exterior vapor barrier, the water retention decreases, but the general rule of thumb is to add a vapor retarder to the warm side during winter of a structure. When placing the vapor retarder on the interior surface, the results show that the retarder decreases the amount of stored moisture in the wall over time (Figure 17). To finalize the correct perm rating, the vapor retarders were assessed in WUFI Bio for mold growth.

Figure 13. Concrete baseline without a vapor retarder.

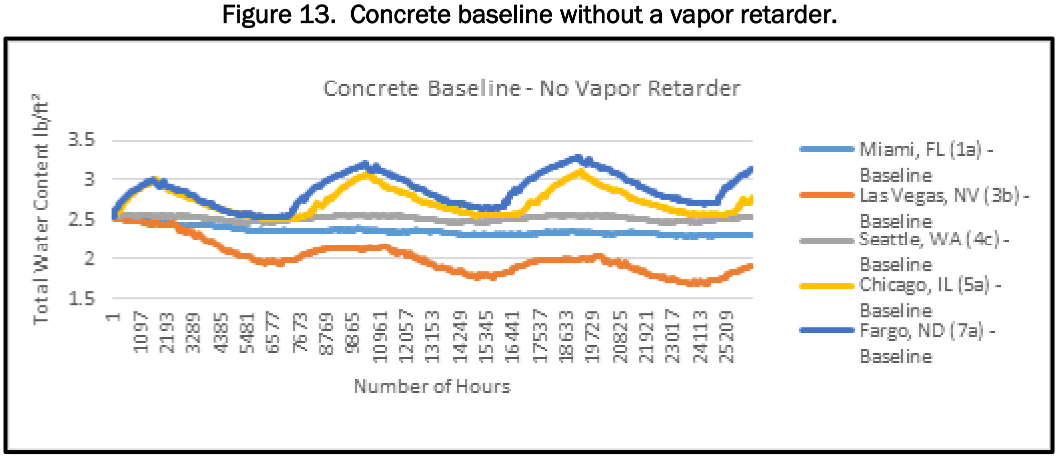

Figure 14. Concrete with vapor retarder of 5.0 perms on exterior.

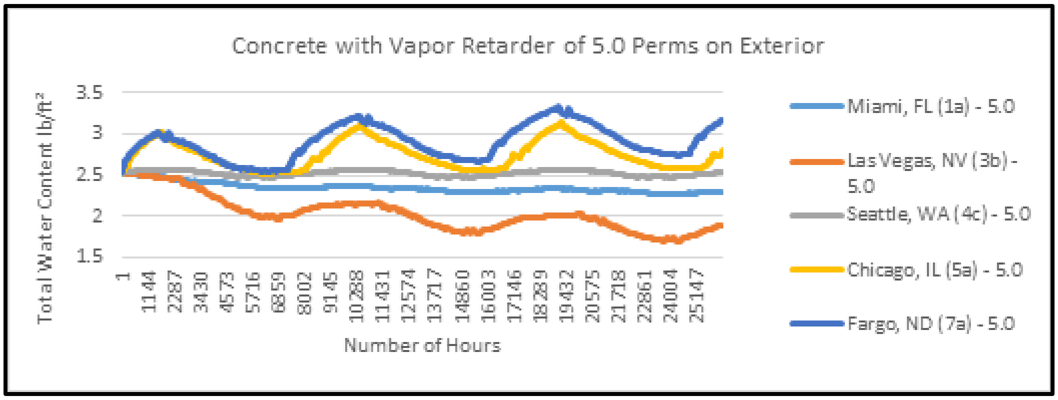

Figure 15. Concrete with vapor retarder of 5.0 perms on interior.

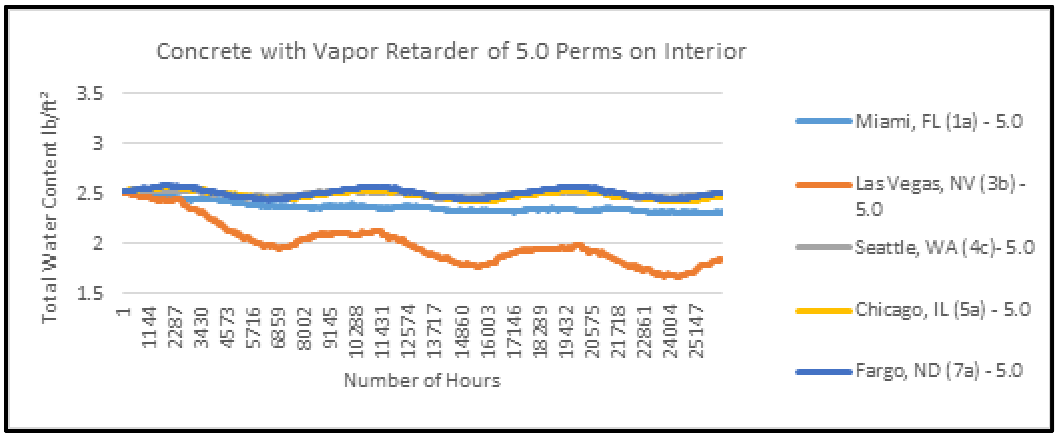

Figure 16. Exterior vapor retarder placement in Chicago, Il (5a)

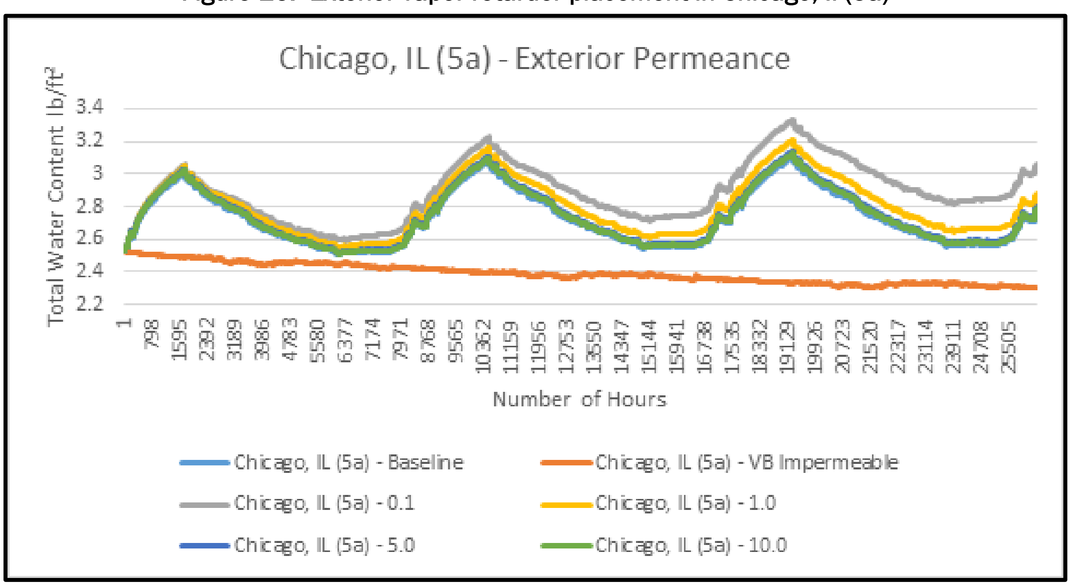

Figure 17. Interior vapor retarder placement in Chicago, Il (5a)

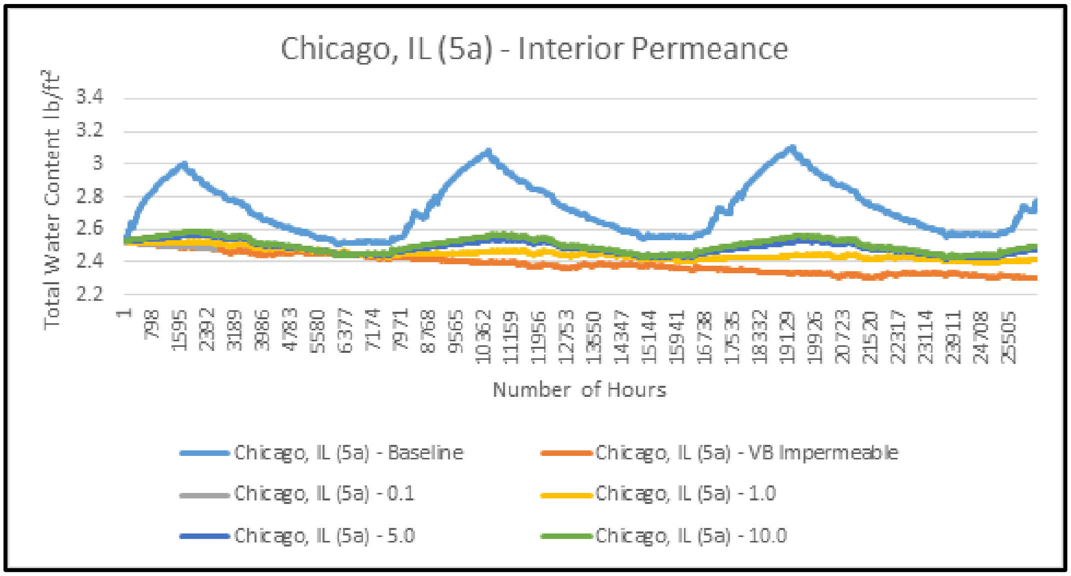

Mold spores can remain active even when a surface has dried (Florian 1992). When the environment becomes conducive to mold growth, the spore begins the germination process. In some cases, spore growth begins when the relative humidity of a space is about 80% at the wall surface, independent of the temperature. Some types of spores can grow in lower humidity (Florian 1992). Figure 18 shows indoor air quality versus relative humidity and its effect on mold spores in the space.

Figure 18. Optimum relative humidity for healthy indoor air.

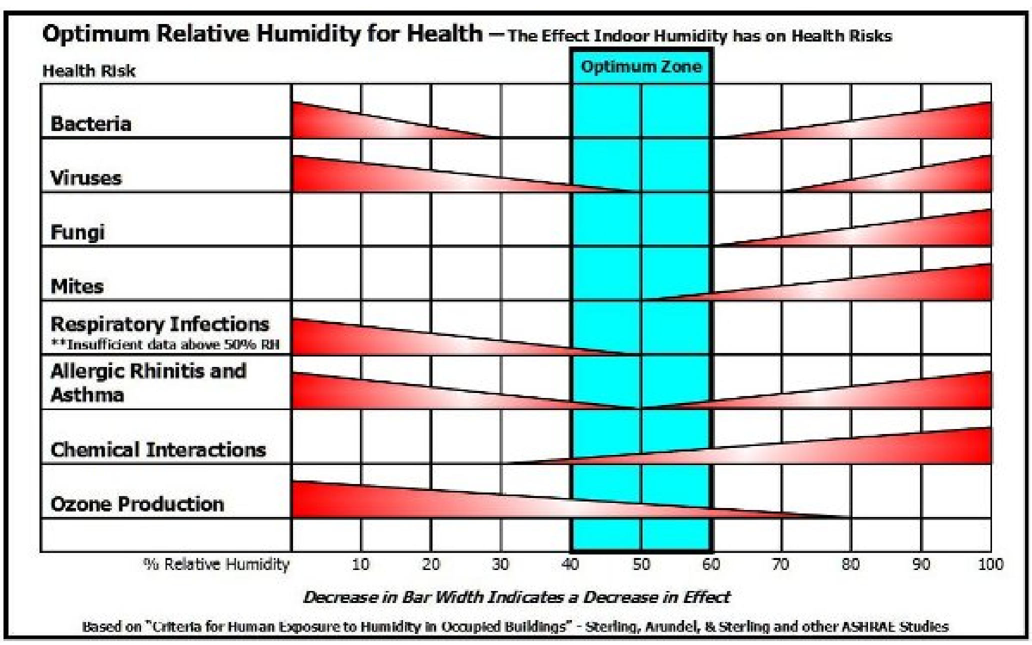

There are also negative health effects associated with relative humidity that is too high or too low. High humidity creates conditions for mold, mildew, and dust mites, all of which can trigger allergic and asthmatic reactions (Schott 2015). When relative humidity is low (i.e., dry), the common cold and flu can become more infectious. It is ideal to maintain relative humidity in the range between 40-60%.

Unlike relative humidity, dewpoint does not depend on the change in air temperature. It is a measurement of the “absolute” amount of water vapor present. Knowing the dewpoint and the temperature at the surface will help predict condensation. When the dewpoint is above the temperature of a cold surface, water vapor will condense. When the dewpoint is below the temperature of surface temperature, it will not. Condensation will occur in other situations such as:

- high temperatures, high relative humidity
- excessively high dewpoints
- unusually cold surfaces
- excessively high dewpoints and cold surfaces
- improper balance between adding/removing water vapor from air (mechanical system)
- building construction
- occupants and activities
- other situations unrelated to the B-Hut design.

The presence of mold is a sign that there is too much moisture in the space. Mold growth requires humidity, a substrate, time, temperature, and unsteady hygrothermal conditions. Figure 19 shows the relative humidity and temperature relative to the germination time of mold. The Lowest Isopleth for Mold is indicated in the right graph, where there is an optimum culture medium for growth.

Figure 19. Germination graph of mold spores.

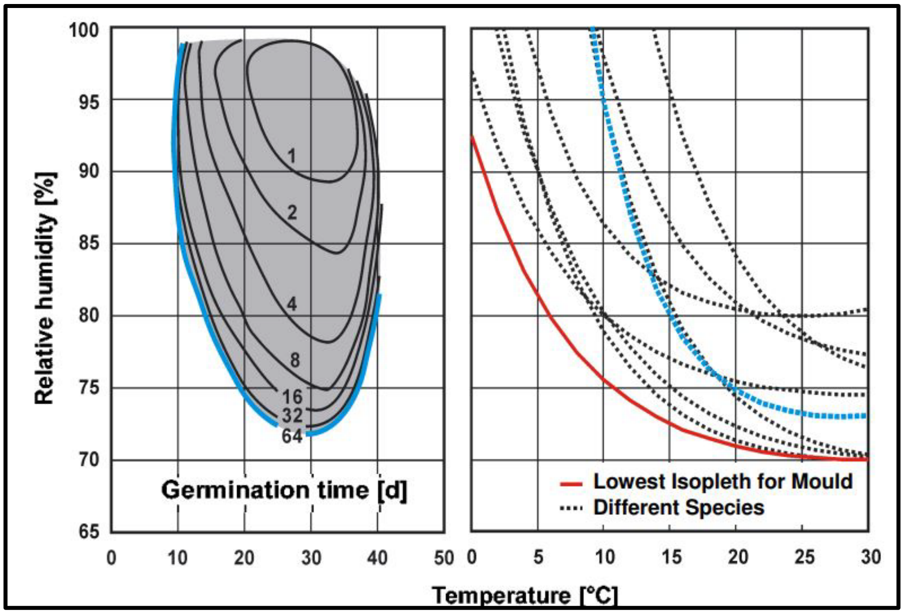

The isopleth diagrams in Figure 20 show the relationship between mold growth, relative humidity, temperature, and the following substrates:

- Substrate Group 0 or LIM 0: Optimal culture medium
- Substrate Group I or LIM I: Biologically recyclable building materials like wall paper, plaster, cardboard, building materials made of biologically degradable raw materials, material for permanent elastic joints
- Substrate Group II or LIM III: Biologically adverse recyclable building materials such as renderings, mineral building material, certain wood as well as insulation material not covered by I
- Substrate Group K: Building materials that are neither degradable nor contain nutrients (most hazardous class).

WUFI® also indicates the growth of mold by relative humidity, temperature and time. Figure 21 displays an isopleth diagram of the B-Hut without a vapor retarder of a Chicago, IL. Figure 22 show the same B-Hut wall using a 1-perm vapor retarder interior wall surface.

Every point in Figures 21 and 22 represents a hygrothermal condition at either the left (exterior) or right (interior) side of the wall sections at a given time. Each color point shows the time that mold growth occurred during the simulation. The colors of the points, which progress from yellow, to darker shades of green, to black, indicate where and how long the mold occurrence appears, and together simulate a long-term trend.

Figure 20. Classification chart of spore germination.

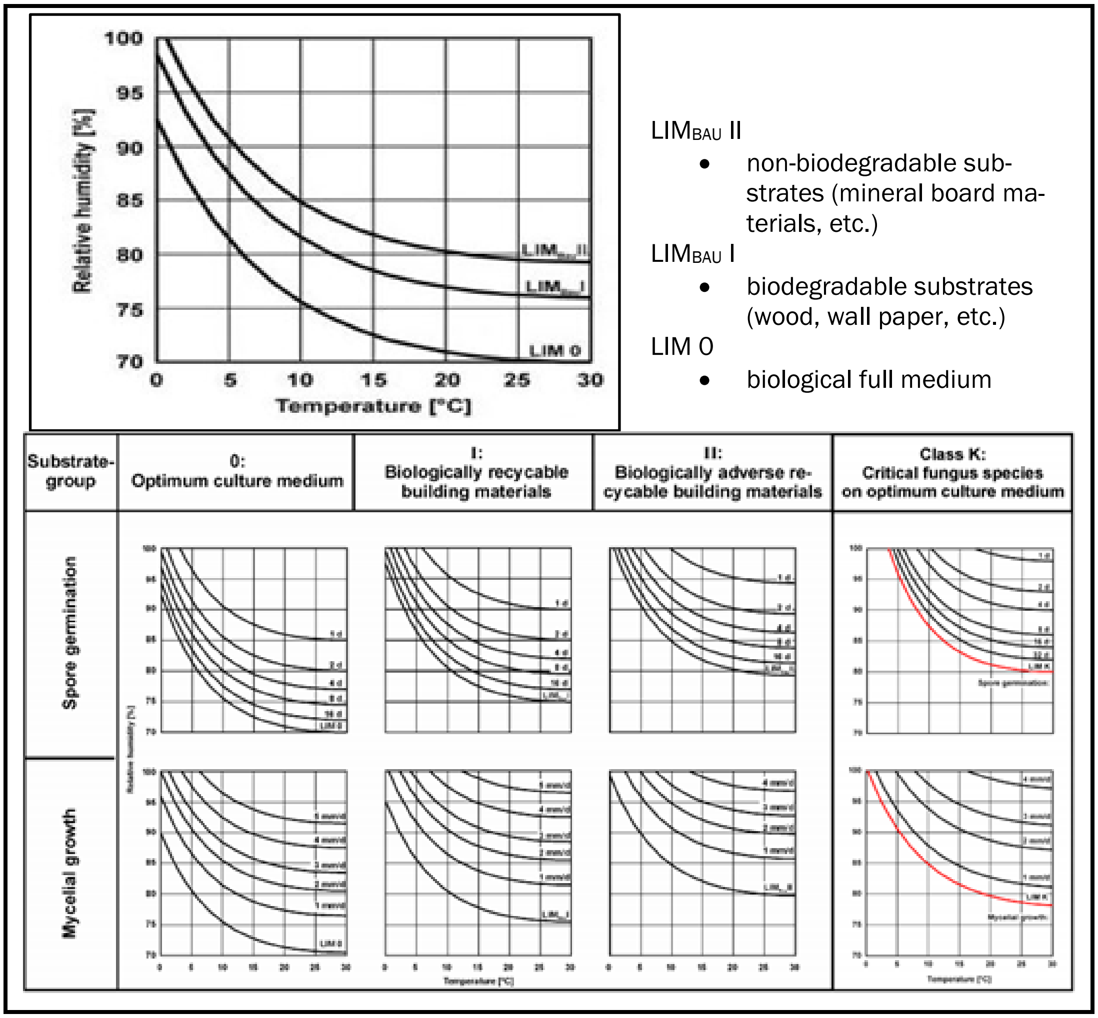

LIM I and LIM II are shown on the graphs that signify the building materials with limiting isopleth. Mold growth is possible if the conditions appear above the limiting isopleth for a long period of time. These graphs are intended to give a quick representation of where mold growth could occur. A more in-depth assessment would require additional information.

In both the baseline graph and the 1.0 perm graph, a relative humidity of approximately 75% and 70˚F will start to show mold growth that are on the LIM I line. The fact that the plotted points in the graphs display an abundant variety of colors (and only some areas show black plot points), indicates that mold occurs more prevalently in the baseline case. In the 1.0 perm case, fewer plotted points are lighter in color.

Figure 21. WUFI® isopleth diagram of the baseline B-Hut wall surface in Climate Zone 5a.

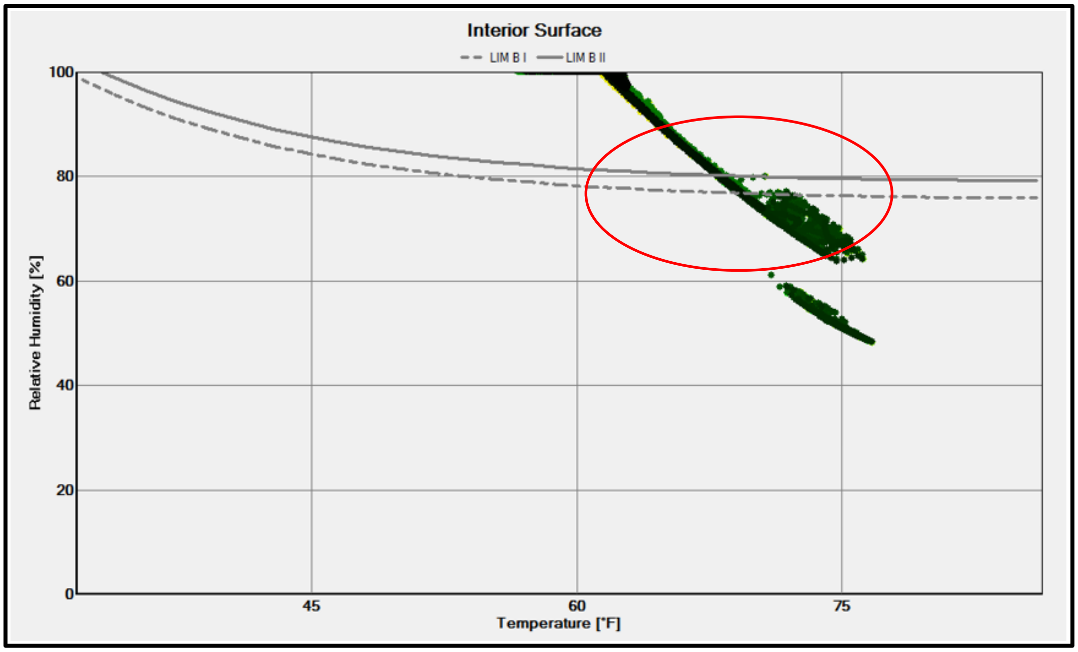

Figure 22. WUFI® isopleth diagram of 1.0 vapor retarder on interior surface in Climate Zone 5a.

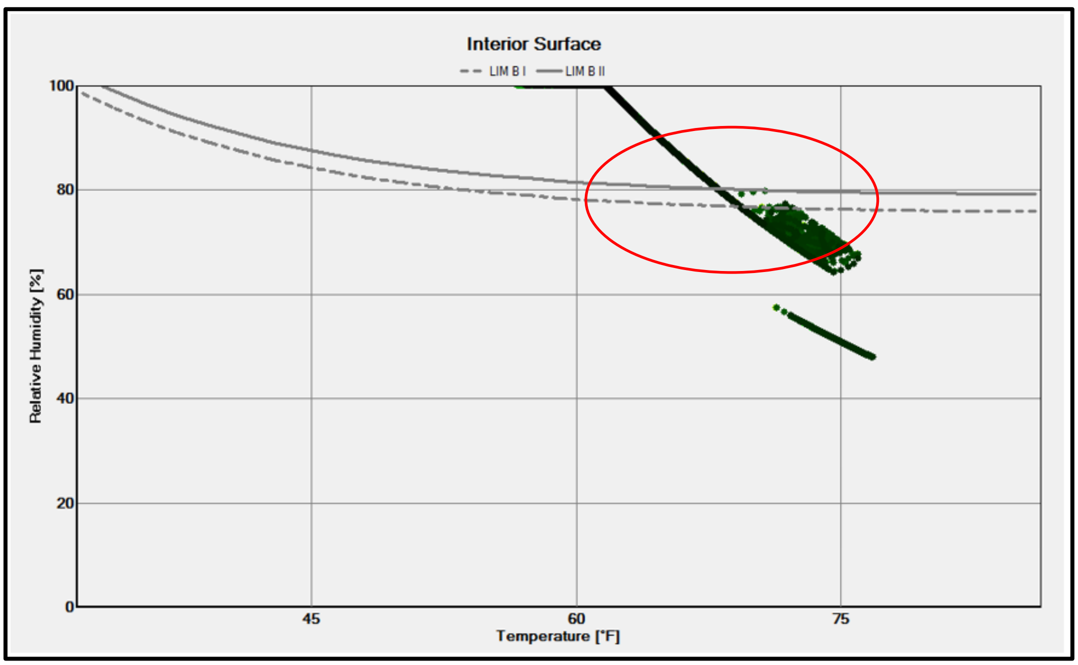

Even though the WUFI® diagram indicates that mold is (theoretically) present, the data were further processed using WUFI® Bio, a biohygrothermal simulator that assesses mold growth under transient hygrothermal boundary conditions. This process compares the measured transient boundary conditions with the growth conditions for typical molds found on building materials. The moisture balance of the mold spores are modeled and compared with the critical water content at which spores would germinate. The increase in class level indicates a harder substrate for microbial growth. WUFI® Bio displays data using "traffic signals" (Figure 23), to indicate whether the wall or roof section passes, falls in the middle, or fails the amount of time that the water content of spores exceeds the critical moisture content of the wall section.

The data in Table 7 indicate whether the type of construction and building material is susceptible to the growth of mold: "y" indicates a passable combination of building materials; "m" indicates the combination of building materials that needs more investigation; and "n" indicates the combination building materials that contain more water content then the critical moisture content for the building material section.

WUFI® Bio displays data using traffic signals to indicate whether the wall or roof section passes, falls in the middle, or fails the amount of time that the water content of spores exceeds (or is similar to) the critical moisture content of the wall section. Figure 24, which shows the results of spore germination relative to the total water content and the critical water content, indicates that, unless the wall is properly dried, mold growth will occur.

Figure 23. Traffic signal indicator in WUFI® Bio.

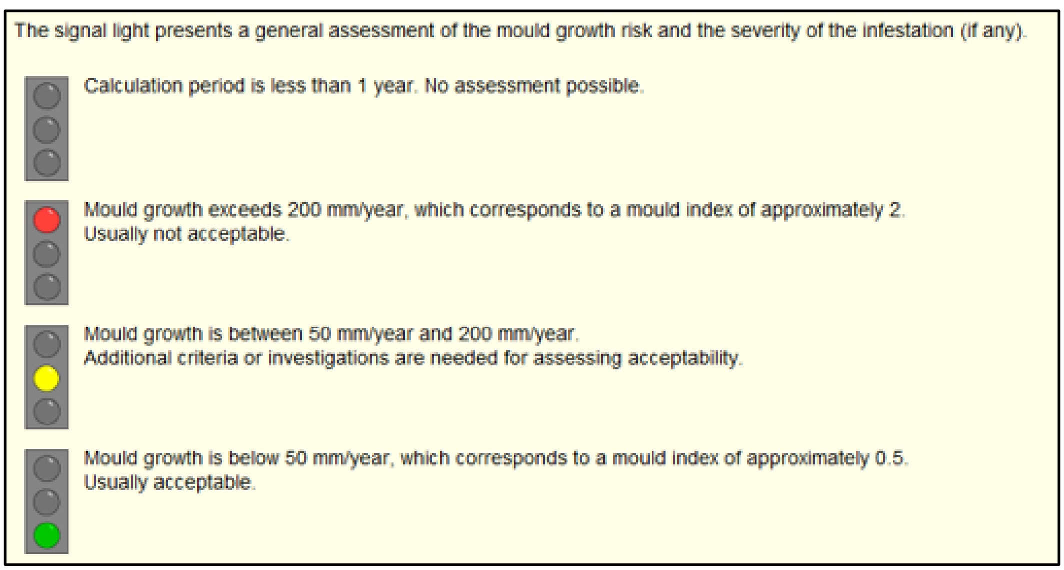

Table 7. Critical moisture content.

Concrete Wall Section - Baseline							
	Year	2013		2014		2015	
	Substrate Group	Class II	Class K	Class II	Class K	Class II	Class K
Location	Miami, FL	Y	Y	Y	Y	Y	Y
	Las Vegas, NV	M	M	M	M	M	M
	Seattle, WA	N	N	N	N	N	N
	Chicago, IL	N	N	N	N	N	N
	Fargo, ND	N	N	N	N	N	N

Figure 24. Mold growth diagram versus time.

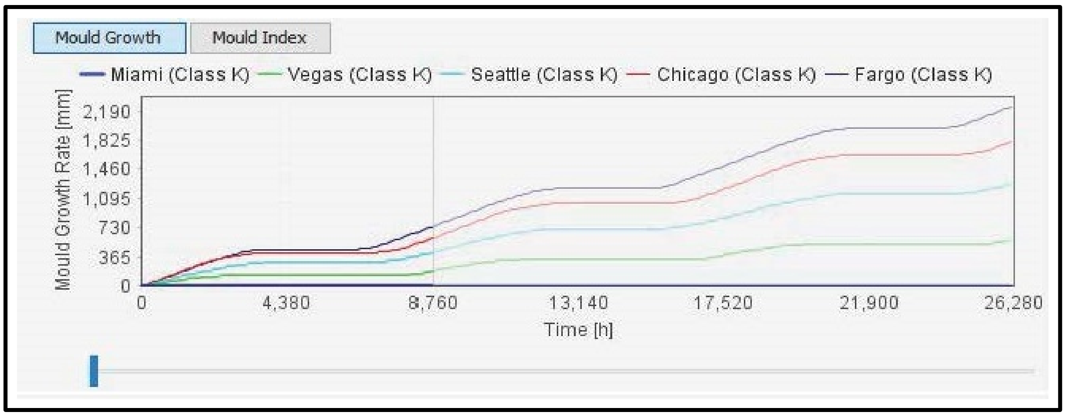

The 1-perm rated vapor retarder data on the interior and exterior surfaces from WUFI® were exported to WUFI® Bio. The traffic signal pattern indication gives a synopsis of the moisture patterns that correlate with the water content of the spore and the critical moisture content (Figure 25). In this case, the exterior and interior both have critical moisture content above the spore's water content in the Climate Zones 4-8, and possibly in Climate Zone 3, with or without a vapor barrier.

The quantification of mold growth is based on the mold index. A mold index uses upper limits that depend on temperature and relative humidity. The WUFI® Mold Index VTT evaluates the intensity of growth using a six-point scale (Table 8).

The WUFI® Mold Index also uses the traffic signal indicator to display these results (Table 9). The traffic patterns tell if the mold is visible either to the naked eye or through a microscope.

Figure 25. Traffic signal indicator in WUFI® Mold Index VTT.

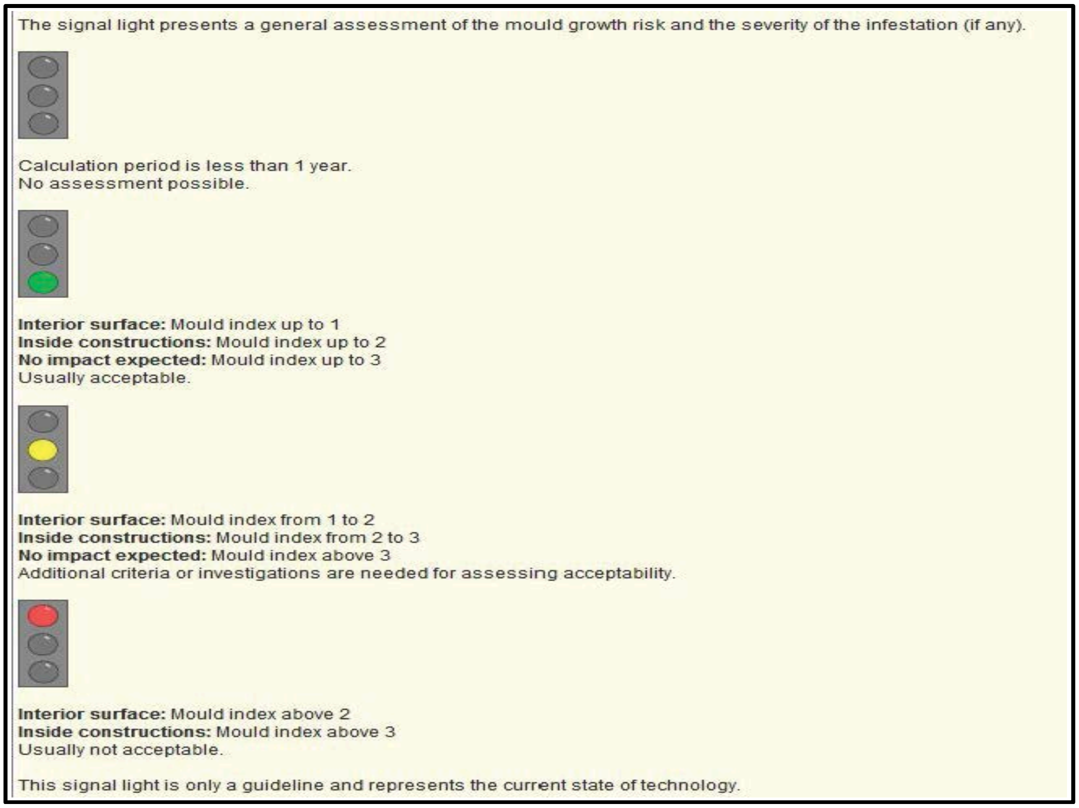

Table 8. Mold index from WUFI® Mold Index VTT.

Mold Index	Description of Growth Rate
0	No growth
1	Small amount of mold on surface (microscope), initial stages of growth
2	Several local mold growth colonies on the surface (microscope)
3	Visual finding of mold on surface, <10 % coverage or <50% coverage of mold (microscope)
4	Visual finding of mold on surface, 10-50% coverage or >50% coverage mold (microscope)
5	Plenty of growth on surface, >50% coverage (visual)
6	Heavy and tight growth, coverage about 100%

Table 9. Traffic signal results from WUFI® Mold Index VTT.

Concrete Wall Section - Baseline				
	Year	2013	2014	2015
Location	Miami, FL	Y	Y	Y
	Las Vegas, NV	Y	Y	Y
	Seattle, WA	Y	Y	Y
	Chicago, IL	N	M	M
	Fargo, ND	N	N	N

Although results indicate that the mold index is above Level 3 in Chicago, IL and Fargo, ND, these results pertain to a concrete wall section that does not included a vented cladding that allows drying for the material; thus, mold growth will occur. The WUFI® Mold Index does consider the fact that mold growth can decrease over time during long dry periods, per ASHRAE Standard 160, *Criteria for Moisture Control Design Analysis in Buildings* (ASHRAE 2016). Limitations of using the WUFI® Mold Index VTT to evaluate the ACES B-Hut construction include the fact that the alkaline conditions of the fresh concrete surface stop the formation of mold, so the mold index values are not valid until carbonation is completed.

2.5.3.3 Conclusion

WUFI® provides a critical capability to identify moisture control issues across walls and roof sections of the 3D-printed concrete B-Hut to eliminate or reduce the issue of mold growth early before construction begins. The analysis of the baseline structure provided a starting point for this process; WUFI® provided the water content and heat and moisture fluxes; WUFI® Bio provided a detailed evaluation of the material's potential to grow mold; and the WUFI® Mold Index VTT generated the mold index of the material's potential to support mold growth.

WUFI® showed that, in warmer climates, walls with lower moisture content will dry at a relatively increased rate. In hotter, humid climates, outdoor relative humidity does not allow interior vapor to escape to the outdoors, resulting in moisture storage in the wall. Incorrect use of vapor barriers will lead to moisture problems. Lstiburek (2004) explains that, while vapor barriers are intended to retard moisture, they can also cause the wall or roof section to dry out. Data results indicate that a vapor barrier consisting of either a spray-applied plastic film or an anti-fungal paint would decrease the stored moisture. Vapor barriers help prevent water vapor in the interior of the house from filtering through the wall and condensing on the warm side of the insulation (RenovateQC 2012).

A vapor barrier combined with an antimicrobial paint should be used as a wall covering. This paint must have the following qualities:

- It must be a water-based fungicidal paint that prevents mold, mildew, and other fungal organisms from thriving.
- It must both cover and kill existing mold moss, algae, fungi, mildew, odor causing bacteria, and any other fungal organisms in B-Hut.

- It must help to cover pre-existing stains and must cover with the appropriate thickness (i.e., mils) to provide the vapor barriers required in specified climate zones.
- It must be able to bond with masonry, metal, and wood.

Two prime factors that influence the selection of construction building materials (i.e., plywood and concrete) are their maintenance requirements and their durability. Overall, plywood is not a favorable building material for B-Huts because it is associated with a host of disadvantages. Plywood is not easily accessible in deployed locations; it must be shipped over long distances. The condition of the product can deteriorate during shipping and storage. When the plywood reaches its destination, an unacceptable amount of the material is wasted in the construction process.

As an organic material, wood is susceptible to mold growth because it provides a food source for germinating spores. Wood also requires sealing or some sort of covering to decrease the amount of moisture stored in the material, and thereby to decrease the health risks associated with damp living spaces, and to improve the durability of the building materials. On the other hand, concrete is a very durable material that can withstand harsh temperatures, whether treated or untreated with protective coating(s). Nevertheless, both plywood and concrete B-Huts require measures to reduce mold growth (to preventing spore activation and germination, and to treat active mold). Figure 26 shows a vapor retarder placement and permeance requirement chart.

2.5.4 Thermal bridges

The term “thermal bridging” refers to the flow of heat from one place to another in a building that has higher than the normal heat flows experienced in other areas of the building. Thermal bridges are material locations, where a material’s properties, geometry, or deficiency allow exceptional heat flow from the building’s interior to exterior or vice versa. Thermal bridges may be caused by poorly installed insulation, discontinuous insulation, balconies, service openings, penetration with other building members (like I-beams), joining roof, slopes where floors and walls meet, edges of windows and doors, and corner junctions.

Figure 26. Vapor barrier chart.

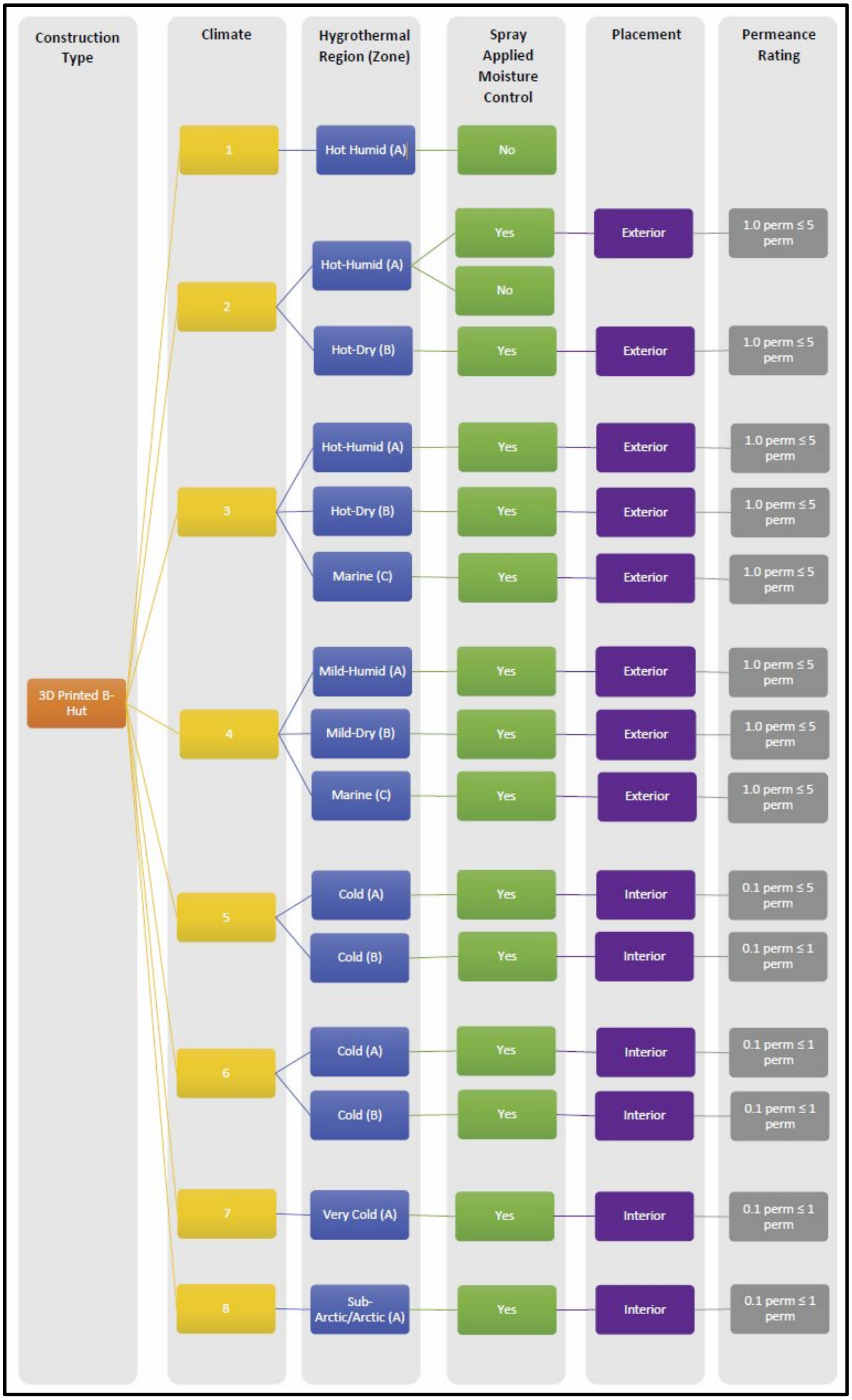

Note: Check with all building codes before applying vapor barrier in specific climate zones.

Thermal bridges convey heat between materials with temperature differences (interior and exterior surfaces) by one or more of three heat transfer modes: conduction, convection, and radiation. Conduction refers to the transfer of energy through a solid material (e.g., metals are more conductive than wood materials). Convection refers to the transfer of energy with the movement of air typically at the surface of wall or roof cavity. Radiation refers to the transfer of energy by a temperature difference where there is no contact between the heat sources or objects, such as the sun transfers energy to the earth. The transfer of energy produces an increase of temperature and continues until the materials reach a steady state (the same temperature) and equilibrium is established. Current building codes have been revised to alleviate the problems caused by thermal bridging (Reynolds 2014).

Thermal bridges contribute to heat loss and therefore increase a building's energy demand. Thermal bridges also increase the risk of condensation occurring at unseen cold spots in walls and roofs, which can then cause health risks and structural integrity problems resulting from mold and mildew (Kore Blog 2016). Overall, thermal bridges, in combination with moisture conditions, can affect a building's air quality, thermal comfort, energy performance, structural integrity, and durability.

To test the thermal properties of the B-Huts, this work performed a thermal study using THERM 7.4, a software program used to study the heat transfer in two-dimension geometry of a building envelope, with or without thermal bridges. THERM is based on numerical methods that use finite element analysis. In THERM, thermal transmittance is expressed using the U-value,* which represents the overall wall conductance and includes wall conduction, surface convection, and radiation.

There are three rules of thumbs to use when specifying R-value, U-value, and thermal resistance:

1. Higher thermal resistances (R-values) of building components are preferred.
2. Lower U-values correspond to higher thermal resistances.

---

* Where U-Value expresses heat transfer through 1 m^2 of a structural element when the difference between the inner and outer face temperature is 1 °F.

3. The U-value is the most accurate way to judge a material's thermal resistance ability, since it takes all heat transfer phenomena into account; however, it is more difficult to predict.

The objective of this work was to obtain a wall construction that would have an R-value of 30 by adding insulation, and to decrease the effects of thermal bridging throughout the wall.

2.5.4.1 Data entry

A 16x8-ft concrete wall resembling that of a cinder block wall, was constructed in THERM on an x-y, two-dimensional plane, with the orientation toward gravity at the ground level, which means that convection will move in the z-direction. Using the material and boundary condition listed in Table 10, the wall is simulated to calculate flux vectors, isotherms, U-value, and other data.

Once these parameters were established, a 12-in. thick concrete block wall was used as the analogue wall section. A concrete baseline of the printed beam was constructed in THERM using the dimension specified by the ACES Team at ERDC-CERL. The wall sections were 16 ft x 8 in., including inside cavities drawn to exact dimensions. After the construction process, both baselines were simulated with air in the cavities. The data listed in Table 10 describe the 12-in. Concrete Block Baseline and the 3D Printed Concrete Wall.

Table 10. Surface unit conductance and unit resistance for air.

Location	Inside	Outside	Cavity
Temperature	70 °F	0 °F	35 °F
Position of Air	Vertical	Wind is 15 mph of 6.5m/s	Any
Direction of Heat Flow	Horizontal	Any	Horizontal
Film Coefficient Btu/hr·ft^2·F	0.43	4.58	*2.51
R (hr·ft^2·F/Btu)	0.68	0.17	*0.27
Emissivity (ε)	0.5	0.5	N/A
U-Factor Surface	Interior	Exterior	N/A
Radiation Model	Auto Enclosure	Blackbody	N/A
Shading System Modifier	None	None	N/A
Blocking Surface	Yes	N/A	N/A

* Values are approximated. The cavity convection value is the average of the inside and outside convection values. The resistance value was calculated using the convections reciprocal. The temperature is an average of the interior and exterior conditions.

The baseline concrete wall was constructed using a modified, lightweight concrete material properties from the THERM Material Library. The concrete wall baseline simulation supplies an overall U-value of the wall with the given boundary condition. A preliminary test of a printed section of the 3D printed wall was done using a Heat Flow Meter at ERDC in Champaign, IL. This test approximated the anticipated thermal conductivity and heat flux of the 3D-printed wall section. This information, along with the concrete wall baseline and assumptions regarding the material properties of the 3D-printed concrete wall were used to model the concrete wall in THERM.

Extrapolating the material properties of lightweight concrete from the concrete wall to the 3D-printed wall gives a baseline for the 3D-printed structure. Figures 27 and 28 show the geometry, flux vectors, and flux magnitudes of both walls. The flux vector shows the direction, strength, and orientation of the heat transfer through the wall sections. Heat flux has direction and magnitude, which make the flux vector a vector quantity, best described through Fourier's Law:

$$\vec{q} = \kappa \nabla T \tag{8}$$

where:

$\vec{q}$ = is the local heat flux density, ($W \cdot m^{-2}$)
κ = the material's conductivity, (W·m-1 K-1)
∇T = the temperature gradient, (K·m-1).

The illustration of heat flux ("Flux Vectors") in Figures 27 and 28 depicts the path of the flux through the wall, depending on the materials characteristics, relative humidity, and temperature changes. Heat flux flows in the direction of the fastest drop in temperature, normal to an isothermal surface, which shows the temperature gradient. The isotherms are lines that show where the temperature was the same at a given time, or on average over a given period.

The data listed in Table 11 detail the overall U-value, including film coefficients, of the wall section without insulation other than the air cavities. Several insulation types were tested using the baseline wall as the basis, providing details about the actions of the U-value. Adding insulation with a low U-value produced lower U-values in the wall section, thus creating higher R-values.

Figure 27. Concrete baseline in THERM.

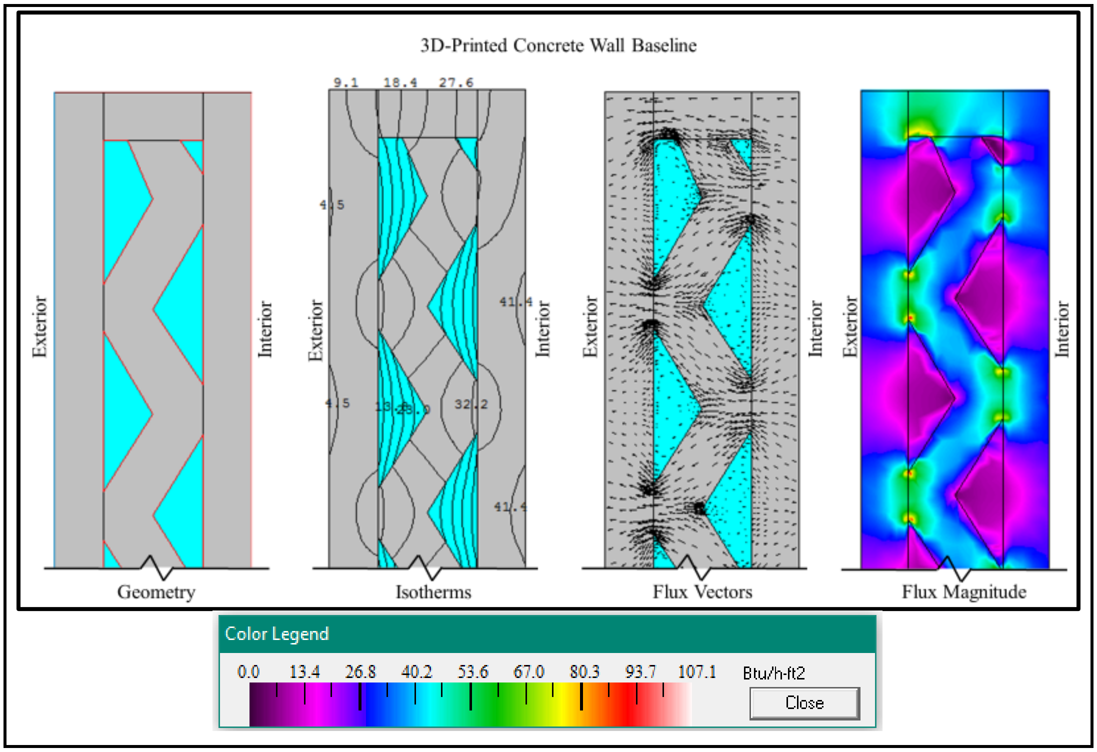

Figure 28. 3D-Printed concrete wall in THERM.

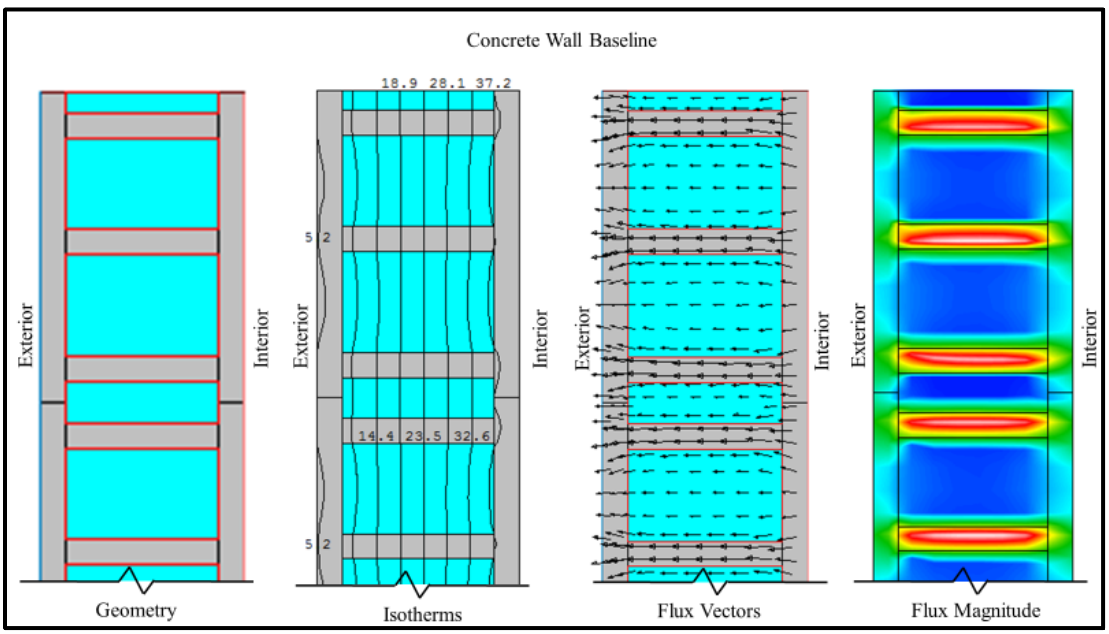

Table 11. Material properties and their overall effect on the U-value on the wall sections.

Insulation Type	Air		Concrete		Perlite		Blown-in Cellulose		Loose-fill Mineral Fiber		Spray-Applied Foam	
Conductance Btu/hr·ft·F	0.05		0.95		0.031		0.024		0.029		0.014	
Emissivity	0.9		0.5		0.9		0.5		0.5		0.9	
*Values	U	R	U	R	U	R	U	R	U	R	U	R
12-in. concrete baseline	0.3823	2.62	0.4938	2.03	0.2795	3.58	0.2757	3.63	0.2785	3.59	0.2695	3.71
3d-printed concrete wall	0.3685	2.71	0.4912	2.04	0.3439	2.91	0.3381	2.96	0.3424	2.92	0.3279	3.05
*[U] U-values units: Btu/hr·ft^2·F, [R] R-value units: hr·ft^2·F/Btu												

Table 11 lists detailed material properties and their overall effect on the U-value and on the wall section. These data, in combination with other considerations, were used to eliminate problematic insulating materials from consideration. Spray-applied foam insulation decreases the overall U-value, thus increasing the R-value. However, at the end of the building's life cycle, the treated building materials would be difficult to recycle because it would be difficult to separate the potentially hazardous spray-applied foam insulation from the concrete rubble that remains. Blown-in cellulose was omitted as a candidate insulation because it could become a food source for mold and insects. Since the thermal conductivity of concrete is greater than that of air, concrete-filled air cavities create a wall section that has little thermal resistance, effectively turning the entire wall section into a thermal bridge. The elimination of spray-applied foam, concrete, and cellulose fiber as insulations left three materials for subsequent testing: Perlite, loose-fill mineral fiber, or air.

2.5.4.2 Data results

After comparing the results of the insulation tests and the effects of insulation on the 3D Printed Concrete Wall section (Table 12), the ERDC-CERL team revised the design of the wall's geometry to include a 1¼-in. troweled exterior, which would reduce the amount of concrete uses and smooth the rough edges (Figure 29). Figure 30 shows the 3D-Printed Concrete Wall with and without the troweled surfaces. This new geometry was constructed in THERM, tested, and compared with the 3D baseline.

Table 12. Simulation results with air film coefficients (simulations with air film coefficients).

		U-Factor Btu/hr·ft²·°F	Heat Flow Btu/hr	Heat Flux Btu/hr·ft²	R-Value hr·ft²·°F/Btu
Air	3D-Printed Concrete Wall	0.3694	414.87	25.93	2.71
	3D-Printed Concrete Wall Troweled	0.3841	431.47	26.97	2.60
Perlite	3D-Printed Concrete Wall	0.3439	386.317	24.14	2.91
	3D-Printed Concrete Wall Troweled	0.3535	397.1	24.82	2.83
Mineral Fiber - Loose-Fill	3D-Printed Concrete Wall	0.3434	384.607	24.04	2.91
	3D-Printed Concrete Wall Troweled	0.3518	395.12	24.69	2.84
Air film coefficients are collected from Table 5-2a Surface Unit Conductance and Unit Resistance for Air adapted from the ASHRAE Fundamental Volume 1989 using assumptions of indoor air film coefficient of 1.46 and outdoor air film coefficient of 6.					

Figure 29. Baseline and proposed wall designs.

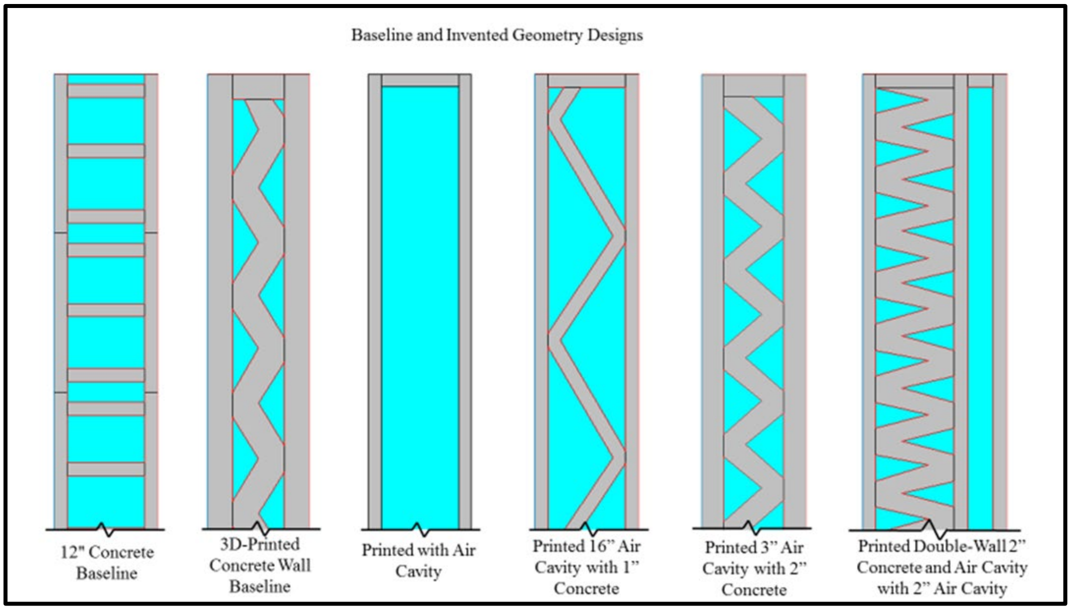

Figure 30. 3D Printed wall troweled with 12-in. exterior cavity, 4-in. interior cavity with 2-in. webbing infill.

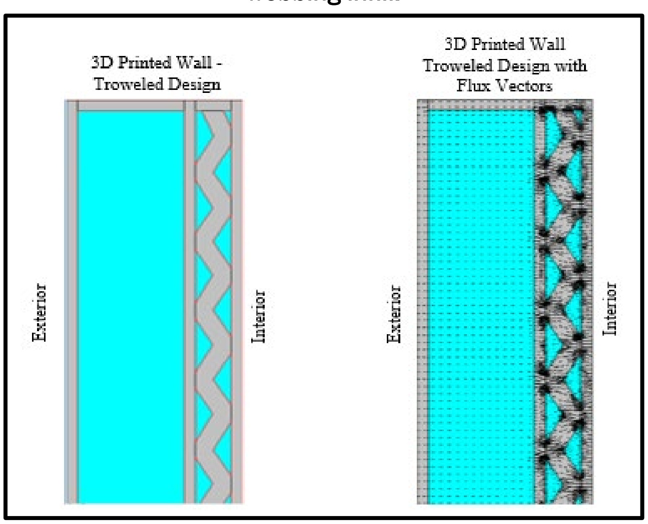

The results indicated there is a loss in R-values when the walls are troweled. After testing the 3D-printed concrete, the ERDC-CERL team again revised the wall's design by increasing the cavity spaces to decrease thermal transmission. This new design was then tested. Results indicated that this modification could potentially increase the cost of insulation to fill the (larger) empty cavities.

A comparison of the U-values of the proposed designs (Table 13) was used to eliminate some designs as printable design candidates, due to their: structural integrity, protection against fire, and ability to print. The incorporation of a bigger air cavity, as shown in the "Printed 3-in. Air Cavity with 2-in. Concrete" and the "Printed 16-in. Air Cavity with 1-in. Concrete" designs show an increase in R-value but would be less buildable due to the size of the cavities.

Table 13. Simulation results for different wall types.

Insulation Type	Air		Concrete		Perlite		Loose-Fill Mineral Fiber	
Conductance (Btu/hr·ft·˚F)	0.05		0.95		0.031		0.029	
Emissivity	0.9		0.5		0.9		0.5	
*Values	U	R	U	R	U	R	U	R
12-in. Concrete Baseline	0.3823	2.62	0.4938	2.03	0.2795	3.58	0.2785	3.59
3D-Printed Concrete Wall	0.3685	2.71	0.4912	2.04	0.3439	2.91	0.3424	2.92
Printed with Air Cavity	0.3274	3.05	0.4912	2.04	0.0657	15.22	0.0628	15.92
Printed 3-in. Air Cavity with 2-in. Concrete	0.3785	2.64	0.4622	2.16	0.334	2.99	0.3325	3.01
Printed 16-in. Air Cavity with 1-in. Concrete	0.2834	3.53	0.4912	2.04	0.1464	6.83	0.1439	6.95
Printed Double Wall 2-in. Air Cavity and Concrete and 2-in. Air Cavity	0.2556	3.91	0.2748	3.64	0.2516	3.97	0.2515	3.98

*[U] U-values units: Btu/hr·ft^2·˚F, [R] R-value units: hr·ft^2·˚F/Btu

2.5.4.3 Conclusion

Any break in the continuity of a thermal barrier creates a thermal bridge. Thermal bridges are hidden paths of heat loss that can cause a host of problems, including increased energy usage, interior condensation, convective loops, air flow problems, etc. In printed concrete construction, thermal bridging can occur throughout an entire beam, but more specifically through any material with higher conductivity. Decreasing the thermal bridge through the beam would decrease heat loss through the wall and roof surfaces to the outside. One way to help manage the thermal bridge through the cement wall is to keep the proposed vapor barrier consistent and continuous, e.g., by avoiding metal fasteners or materials that will act as thermal bridges through the wall. It is important to manage thermal bridges by maintaining continuous insulation because this directly improves the building's energy efficiency and controls condensation.

Since the B-Hut must be made from recyclable materials, to ease demolition to gravel at the end of the building's life cycle, the use of spray foam as an insulation was infeasible. Cellulose was also eliminated from consideration since it acts as a spore substrate that could stimulate mold growth within the wall structure. Also, results indicated that is not possible to achieve the proposed insulation values of R-15 to R-30 with the cavities filled with air (Table 14). However, it was determined that perlite and a loose-fill mineral fiber would be sufficient insulators, and that it may be possible to reach higher R-values with by filling the printed wall's interior air cavity with perlite or mineral fiber. After these tests, the double wall geometry was determined to be the most likely candidate for printed wall geometry, but only if the actual thermal conductivity improves in the overall wall section.

Table 14. Simulation results with varying cavity sizes (original geometry with interior air gap simulations with air film coefficients).

ORIGINAL GEOMETRY WITH INTERIOR AIR GAP SIMULATIONS WITH AIR FILM COEFFICIENTS							
		Cavity Size					
	Wall Types	4”		8"		12"	
Insulation Type	*Values	U	R	U	R	U	R
Air	3D-Printed Concrete Wall	0.2216	4.51	0.2201	4.54	0.2225	4.49
	3D-Printed Concrete Wall Troweled	0.22294	4.49	0.2285	4.38	0.2312	4.33
Perlite	3D-Printed Concrete Wall	0.0877	11.40	0.0535	18.69	0.0389	25.71
	3D-Printed Concrete Wall Troweled	0.0852	11.74	0.0502	19.92	0.0358	27.93
Mineral Fiber	3D-Printed Concrete Wall	0.0847	11.81	0.0561	17.83	0.0375	26.67
	3D-Printed Concrete Wall Troweled	0.0819	12.21	0.0483	20.70	0.0344	29.07
*[U] U-values units: Btu/hr·ft²·˚F, [R] R-value units: hr·ft²·˚F/Btu							

2.6 Conclusion

This work concludes that a comprehensive analysis of the building envelope, including thermal bridges, moisture, airflow and heat transfer is very important to deliver an integrated solution. Studying each component individually will not provide an adequate solution. More concise, pinpointed data-driven information will further enhance B-Hut construction with technologies that may extend to other types of construction as well.

3 Summary and Recommendations

3.1 Summary

The U.S. Department of Defense is striving to meet the critical structural needs at contingency bases sustainably by improving the efficiencies of construction, maintenance, and operation. The U.S. Army (HQDA 2010) has likewise stated that such sustainability "is primarily achieved through reduced demand and cost-effective consumption of resources." To achieve these goals, this work undertook to develop a construction process that reduces the amount of manpower needed for construction, reduces the quantity of materials required to build and maintain structures, and reduces energy consumption (and lowers costs of operation).

The "B-Hut" is one common structure the military builds at contingency bases for administrative, operations, and living facilities. The B-Hut must provide the Warfighter with two key elements: thermal comfort (the building must remain warm and dry, free of precipitation and condensation), and optimal force protection (the building must provide a secure shelter with structural integrity). Construction techniques for the B-Hut currently involve labor- and resource-intensive construction practices. Yet many construction processes are similar in type and complexity to manufacturing processes that already use robotics and automated systems.

This research developed and evaluated the capability to perform construction using an automated, additive concrete construction process using locally available materials. This fabrication technology uses computer control to exploit the surface-forming capability of troweling to create smooth and accurate planar and freeform surfaces out of extruded materials at a construction scale.

The use of concrete as a construction material provides a safe, secure, tough exterior as well as thermal comfort to the Warfighter. The process prevents inconsistencies in materials or insulation to preclude thermal bridging, which might otherwise add to the thermal heat gain throughout the wall or roof system. Robotic construction also permits automated application of camouflage, concealment, and deception strategies to structures as they are constructed.

The use of local materials as the primary source for construction material will greatly reduce the availability and time-to-use of the material, and also allows the design and construction of buildings that are: (1) similar to existing architecture in appearance and aesthetic value, (2) more acceptable for subsequent use by the host population, (3) better understood by the local population, and (4) easily supplied with maintenance and repair materials.

3.2 Recommendations

To ensure minimum air and moisture infiltration, it is recommended to seal gaps and cracks, especially around doors and windows when applicable. Any connection member (i.e., door, roof) should be properly installed to reduce air and moisture infiltration. With the current geometric 3D print of the B-Hut, the concrete itself is an adequate barrier. The roof interface to the roofing structure, however, needs an air barrier. Thermal bridges could occur in these spaces producing an environment for mold growth due to condensation. To avoid heat fluxes through thermal bridging, it is recommended to use materials with low conductivity for reinforcement.

Use the appropriate HVAC system to remove humidity when needed. Consider the dewpoint of the air in the interior to prevent condensation from forming. Using a thermostat to maintain the conditions inside the B-Hut can save on heating and cooling cost when operating correctly. Programmable thermostats can be adjusted to pre-set schedules. The thermostat system should be properly synchronized with the HVAC system used in the B-Hut. The indoor environment must also be properly vented.

The type of vapor retarder required depends on the outdoor temperatures and relative humidity, and on the construction materials. Therefore, ASHRAE Standard 189.1 requires that calculations be performed to demonstrate that conditions conducive to condensation within the building envelope do not occur.

Insulation should be used in the cavities to decrease the overall U-value of the wall (Table 15). Mineral fiber has an R-value of 2.8 $hr \cdot ft^2 \cdot {}^\circ F/Btu$ while perlite is 2.7 $hr \cdot ft^2 \cdot {}^\circ F/Btu$. Adding either one of these insulations will decrease the heat through the wall or roof. Thermal bridging can be further avoided if the B-Hut design has geometry that improves the R-value without the addition of insulation. Use paint or sealant as a vapor barrier in the appropriate locations (see Figure 26 or Table 16). Antimicrobial fungicide should be included in the spray-applied paint or sealant. The concrete wall coating must have two coats of paint or sealer.

Table 15. Building envelope for insulation for mass walls, roofs, and floors.

		1 (A, B)		2 (A, B)		3 (A, B, C)		4 (A, B, C)	
	Value	U	R	U	R	U	R	U	R
Residential	Roof	0.027	38	0.027	38	0.027	38	0.019	60
	Wall	0.151	5.7	0.123	7.6	0.104	9.5	0.081	13
	Floor	0.322	NR	0.087	8.3	0.074	10	0.046	18.7
Commercial	Roof	0.027	38	0.027	38	0.027	38	0.019	60
	Wall	0.58	NR	0.151	5.7	0.123	7.6	0.094	11.4
	Floor	0.322	NR	0.107	6.3	0.074	10	0.051	16.7
		5 (A, B)		6 (A, B)		7 (A)		8 (A)	
	Value	U	R	U	R	U	R	U	R
Residential	Roof	0.019	60	0.019	60	0.015	71	0.015	70
	Wall	0.072	15.2	0.064	19.6	0.064	19.6	0.043	22
	Floor	0.046	18.7	0.046	18.7	0.038	25.1	0.034	27.2
Commercial	Roof	0.019	60	0.019	60	0.015	71	0.015	71
	Wall	0.081	13	0.072	15.2	0.064	19.6	0.043	22
	Floor	0.051	16.7	0.046	18.7	0.038	25.1	0.034	27.2

U-value is the assembly's maximum, units: Btu/hr·ft^2·˚F.
R-value is insulation minimum, units: hr·ft^2·˚F/Btu.
Adapted from ASHRAE Standards 189.1 in Imperial Units

Table 16. Vapor barrier flow.

Construction Type	Climate	Hygrothermal Region (Zone)	Spray-Applied Moisture Control	Placement	Permeance Rating
3D Printed B-Hut	1	A	No	N/A	N/A
	2	A	Yes	Exterior	1.0 perm ≤ 5.0 perm
		A	No	See note	Check with Standard
		B	Yes	Exterior	1.0 perm ≤ 5.0 perm
	3	A	Yes	Exterior	1.0 perm ≤ 5.0 perm
		B	Yes	Exterior	1.0 perm ≤ 5.0 perm
		C	Yes	Exterior	1.0 perm ≤ 5.0 perm
	4	A	Yes	Exterior	1.0 perm ≤ 5.0 perm
		B	Yes	Exterior	1.0 perm ≤ 5.0 perm
		C	Yes	Exterior	1.0 perm ≤ 5.0 perm
	5	A	Yes	Interior	0.1 perm ≤ 5.0 perm
		B	Yes	Interior	0.1 perm ≤ 1.0 perm
	6	A	Yes	Interior	0.1 perm ≤ 1.0 perm
		B	Yes	Interior	0.1 perm ≤ 1.0 perm
	7	A	Yes	Interior	0.1 perm ≤ 1.0 perm
	8	A	Yes	Interior	0.1 perm ≤ 1.0 perm

Table 17 lists calculated design temperature associated with the different cavity sizes. This listing can help determine the size cavity to use for specific types of walls insulation, or to meet specific building codes. The (heating and cooling) degree day (HDD and CDD) measure was used only to approximate the climate zones average temperature in the THERM simulation test. If loose-fill insulation is used, the cavity must be filled in its entirety.

The building insulation listed in Table 17 may be used to perform quick calculations to predict the wall cavity size to house the insulation in each climate zone. Mineral fiber slightly improved the U-value of the wall in comparison to the perlite, but either could be used in the insulation application.

Table 17. U- and R-values for each climate zone.

U- and R-values for Thermal Criteria												
Size of Cavity Space	4 in.				8 in.				12 in.			
Thermal Conditions	CDD		HDD		CDD		HDD		CDD		HDD	
Values	U	R	U	R	U	R	U	R	U	R	U	R
Perlite	0.0766	13.05	0.0766	13.05	0.0469	21.32	0.0469	21.32	0.0341	29.33	0.0341	29.33
Mineral Fiber	0.074	13.51	0.074	13.51	0.0452	22.12	0.0452	22.12	0.0327	30.58	0.0328	30.49

Results using 85˚F for outdoor air temperature, 72˚F indoor air temperature for CDD and 10˚F for outdoor air temperature, 75˚F indoor air temperature for HDD.

*[U] U-values units: Btu/hr·ft^2·˚F, [R] R-value units: hr·ft^2·˚F/Btu

Bibliography

Cited works

American Society of Heating, Refrigerating, and Air-Conditioning Engineers (ASHRAE). 2016. *Criteria for Moisture-Control Design Analysis in Buildings*. ASTM 160. West Conshohocken, PA: ASTM International, DOI: 10.1520/C0078-10e1.

de Dear, R. J., and Brager, G. S. 2002. "Thermal Comfort in Naturally Ventilated Buildings: Revisions to ASHRAE Standard 55." *Energy and Buildings* 34(6), 549-561.

Department of Army. 2008. Army Regulation 420–1. *Facilities Engineering Army Facilities Management*. Washington, DC: Headquarters, Department of the Army (HQDA).

Florian, Mary Lou. 1992. What It Takes to Activate a Fungal Spore: An Excerpt from the Guldbeck Memorial Lecture. *Abbey Newsletter* 16(1). http://cool.conservation-us.org/byorg/abbey/an/an16/an16-1/an16-116.html.

HQDA (Headquarters, Department of the Army). 2010. *Base Camps*. ATP 3-37.10/MCRP 3-17.7N. Washington DC: HQDA. http://www.marines.mil/Portals/59/MCRP%203-17.7N%20z.pdf.

HQTRADOC) Headquarters, U.S. Army Training and Doctrine Command). 2009. *United States Army TRADOC Analysis Center*. TRADOC Regulation 10-5-7. Fort Monroe, VA: TRADOC

International Code Consortium. 2006. *International Energy Conservation Code.* Washington, DC: U.S. Department of Energy.

Kore Blog. 2016. *Concrete Vapor Barriers: Critical Building Protection*. https://www.wrmeadows.com/concrete-vapor-barriers/.

Lstiburek, J. W. 2004. "Understanding Vapor Barriers." *ASHRAE Journal* 46(8):40.

Lstiburek, J., and J. Carmody. 1996. *Moisture Control Handbook: Principles and Practices for Residential and Small Commercial Buildings*. New York: John Wiley & Sons.

Mullen, M. G. 2011. *National Military Strategy of the United States of America*. Government Printing Office.

Obama, B. 2010. *National Security Strategy of the United States: 2011, Redefining America's Military Leadership*. Washington, DC: Chairman, Joint Chiefs of Staff, https://www.army.mil/e2/rv5_downloads/info/references/NMS_Feb2011.pdf.

RenovateQC. 2012. "Vapor Barriers - to Install or Not?" *RenovateQC: Local Solutions for Restoring Your Historic Home*. http://renovateqc.org/node/179.

Reynolds, M. 2014. *What Is a Thermal Bridge and Why Is It So Important to Break It?* http://www.ecohome.net/guide/thermal-bridge-important-break.

Schott, B. 2015. *Controlling Your Home's Humidity Means Fewer Allergy and Asthma Triggers*. https://breatheeasyhome.org/controlling-your-homes-humidity-means-fewer-allergy-and-asthma-triggers/.

TenWolde, A., and C. L. Pilon. 2007. "The Effect of Indoor Humidity on Water Vapor Release in Homes." *Proceedings, ASHRAE Thermal Performance of the Exterior Envelopes of Whole Buildings X* (December 2-7 2007). Atlanta, GA: ASHRAE. http://web.ornl.gov/sci/buildings/conf-archive/2007%20B10%20papers/071_TenWolde.pdf.

Uncited works

ACI (American Concrete Institute). 2009. *Standard Practice for Selecting Proportions for Normal, Heavyweight, and Mass Concrete*. ACI 211.1-91 (R2009). Farmington Hills, MI: ACI Committee 211.

ASHRAE. 2004a. *Ventilation for Acceptable Indoor Air Quality*. Standard 62.1-2004. Atlanta, GA: ASHRAE.

———. 2004b. *Energy Standard for Buildings Except Low-Rise Residential Buildings*. American National Standards Institute (ANSI), ASHRAE, and the Illuminating Engineering Society of North America (IESNA) Standard 90.1-2004. Atlanta, GA: ASHRAE.

ASTM (American Society for Testing and Materials). 2008. *Standard Test Method for Time of Setting of Concrete Mixtures by Penetration Resistance*. ASTM C403. West Conshohocken, PA: ASTM International.

———. 2009. *Standard Test Method for Drying Shrinkage of Mortar Containing Hydraulic Cement*. ASTM C596. West Conshohocken, PA: ASTM International.

———. 2010. *Standard Test Method for Flexural Strength of Concrete (Using Simple Beam with Third-Point Loading)*. ASTM C78. West Conshohocken, PA: ASTM International.

———. 2011. *Standard Practice for Use of Apparatus for the Determination of Length Change of Hardened Cement Paste, Mortar, and Concrete*. ASTM C490. West Conshohocken, PA: ASTM International.

———. 2011. *Standard Test Method for Splitting Tensile Strength of Cylindrical Concrete Specimens*. ASTM C496. West Conshohocken, PA: ASTM International.

———. 2012a. *Standard Specification for Portland Cement*. ASTM C150. West Conshohocken, PA: ASTM International.

———. 2012b. *Standard Test Method for Slump of Hydraulic-Cement Concrete*. ASTM C143. West Conshohocken, PA: ASTM International.

———. 2013a. *Standard Specification for Concrete Aggregates*. ASTM C33. West Conshohocken, PA: ASTM International.

———. 2013b. *Standard Specification for Chemical Admixtures for Concrete*. ASTM C494. West Conshohocken, PA: ASTM International.

———. 2013c. *Standard Test Method for Compressive Strength of Hydraulic Cement Mortars (Using 2-in. or [50-mm] Cube Specimens)*. ASTM C109. West Conshohocken, PA: ASTM International.

———. 2013c. *Standard Test Methods for Time of Setting of Hydraulic Cement by Vicat Needle*. ASTM C191-13. West Conshohocken, PA: ASTM International, DOI: 10.1520/C0191-13.

———. 2013d. *Standard Test Method for Flow of Hydraulic Cement Mortar*. ASTM C1437. West Conshohocken, PA: ASTM International.

———. 2013d. *Standard Test Method for Compressive Strength of Hydraulic Cement Mortars (Using 2-in or [50-mm] Cube Specimens)*. ASTM C109-13. West Conshohocken, PA: ASTM International, DOI: 10.1520/C0109-13.

———. 2013e. *Standard Test Method for Flow of Hydraulic Cement Mortar*. ASTM C1437-13. West Conshohocken, PA: ASTM International, DOI: 10.1520/C1437-13.

———. 2014. *Standard Specification for Flow Table for Use in Tests of Hydraulic Cement*. ASTM C230-14. West Conshohocken, PA: ASTM International, 10.1520/C0230-14.
Superseded by Active Standard ASTM C78/C78M.
http://compass.astm.org/Standards/HISTORICAL/C78C78M-10.htm.

———. 2014. *Standard Terminology Relating to Concrete and Concrete Aggregates*. ASTM C125. West Conshohocken, PA: ASTM International.

———. 2016a. *Criteria for Moisture-Control Design Analysis in Buildings*. ASTM 160. West Conshohocken, PA: ASTM International, DOI: 10.1520/C0078-10e1.

———. 2016b. *Standard Test Method for Flexural Strength of Concrete (Using Simple Beam With Third-Point Loading)*. ASTM C78-10. West Conshohocken, PA: ASTM International, DOI: 10.1520/C0078-10e1.

BASF. 2014. *MasterSet R 100Technical Data Sheet*. Cleveland, OH: BASF Corporation.

———. 2015a. *MasterGlenium 7500 Technical Data Sheet*. Cleveland, OH: BASF Corporation.

———. 2015b. *MasterGlenium 7700 Technical Data Sheet*. Cleveland, OH: BASF Corporation.

———. 2015c. *MasterLife SRA 20Technical Data Sheet*. Cleveland, OH: BASF Corporation.

———. 2015d. *MasterMatrix 33 Technical Data Sheet*. Cleveland, OH: BASF Corporation.

———. 2015e. *MasterSet FP 20 Technical Data Sheet*. Cleveland, OH: BASF Corporation.

Bentur, A., S. Diamond, and S. Mindess. 1985. "The Microstructure of Steel Fibre-Cement Interface." *Journal of Materials Science* 20(10):3610-3620.

Bentur, A., and S. Mindess. 2007. *Fibre Reinforced Cementitious Composites*. New York, NY: Taylor and Francis.

Caltrans (State of California Department of Transportation). 2010. *Guidelines for the Design & Inspection of Concrete*. Sacramento, CA: Caltrans.

Cesaretti, G., E. Dini, X. De Kestelier, V. Colla, and L. Pambaguian. 2013. "Building Components for an Outpost on the Lunar Soil by Means of a Novel 3D Printing Technology." *Acta Astronautica* 93:430-450, DOI 10.1016/j.actaastro.2013.07.034.

Daniel, D. G. 2006. "Factors Influencing Concrete Workability." In J. Lamond and J. H. Pielert (eds.). *Significance of Tests and Properties of Concrete and Concrete-Making Materials*. STP 169D. West Conshohocken, PA: American Society for Testing and Materials.

Di Carlo, T. 2012. *Experimental and Numerical Techniques to Characterize Structural Properties of Fresh Concrete Relevant to Contour Crafting*. PhD Dissertation. Los Angeles, CA: USC.

DOE (U.S. Department of Energy). 2008. *EnergyPlus, Building Energy Simulation Software*. Web site. Washington, DC: DOE.

Emmerich, Steven J., and Andrew K. Persily. 2014. "Analysis of U.S. Commercial Building Envelope Air Leakage Database to Support Sustainable Building Design." *International Journal of Ventilation* 12(4):331-344.

Ferraris, C. F., and F. de Larrard. 1998. "Modified Slump Test to Measure Rheological Parameters of Fresh Concrete." *Cement, Concrete, and Aggregates, CCAGDP* 20(2):241-247.

Ferraris, C., F. de Larrard, and N. Martys. 2001. "Fresh Concrete Rheology: Recent Developments." In Sidney Mindess and Jan Skalny (eds.). *Material Science of Concrete VI*. Westerville, OH: The American Ceramic Society, pp 215-241.

Givoni, Baruch. 1992. "Comfort, Climate Analysis and Building Design Guidelines." *Energy and Buildings* 18(1):11-23.

Goodwin, F. 2006. Volume change. In J. Lamond and J.H. Pielert (eds.). *Significance of Tests and Properties of Concrete and Concrete-Making Materials*. STP 169D. West Conshohocken, PA: ASTM.

Hassen, K. E., J. G. Cabrera, and R. S. Maliehe. 2000. "The Effect of Mineral Admixtures on the Properties of High-Performance Concrete." *Cement and Concrete Composites* 22(4):267-271.

Herron, D., A. Zhivov, and M. Deru. 2009. "Energy Design Guides for Army Barracks." *ASHRAE Transactions* 115(2):984-996.

Jolin, M., D. Burns, B. Bissonnette, F. Gagnon, and L-S. Bolduc. 2009. "Understanding the Pumpability of Concrete." *Proceedings Shotcrete for Underground Support XI*. Davos, Switzerland: Engineering Conferences International. http://dc.engconfintl.org/cgi/viewcontent.cgi?article=1009&context=shotcrete.

Keating, S., N. A. Spielberg, J. Klein, and N. Oxman. 2014. "A Compound Arm Approach to Digital Construction." *Robotic Fabrication in Architecture, Art and Design*, pp 99-110. DOI 10.1007/978-3-319-04663-1_7. http://link.springer.com/chapter/10.1007%2F978-3-319-04663-1_7#page-1

Khoshnevis, B. 1999. "Contour Crafting: State of Development." *Proceedings of the Solid Freeform Fabrication Symposium*. Austin, TX: University of Texas, pp 743-750.

Khoshnevis, B., D. Hwang, K-T. Yao, and Z. Yeh. 2006 "Mega-Scale Fabrication by Contour Crafting." *International Journal of Industrial and Systems Engineering* 1(3):301–320.

Kim, H. K., D. D. Cortes, and J. C. Santamarina. 2007. "Flow Test: Particle-Level and Macroscale Analyses." *ACI Materials Journal* 104(3).

Korhonen, C. J., P. M. Seman, and L. A. Barna. 2004. *Extending the Season for Concrete Construction and Repair, Phase I – Establishing the Technology*. ERDC/CRREL TR-04-02. Hanover, NH: Engineer Research and Development Center, Cold Regions Research and Engineering Laboratory (ERDC-CRREL).

Kosmatka, S. H., B. Kerkhoff, and W. C. Panarese. 2003. *Design and Control of Concrete Mixtures, EB001*. 14th ed. Skokie, IL : Portland Cement Association.

Kucharska, L., and M. Moczko. 1994. "Influence of Silica Fume on the Rheological Properties of the Matrices of High-Performance Concretes." *Advances in Cement Research* 6(4):139-145.

Le, T. T., S.A. Austin, S. Lim, and R. A. Buswell. 2012a. "Mix Design and Fresh Properties for High-Performance Printing Concrete." *Materials and Structures* 45(8):1221-1232. DOI 10.1617/s11527-012-9828-z.

Le, T. T., A. Austin, S. Lim, R. A. Buswell, R. Law, A. G. F. Gibb, and T. Thorpe. 2012b. "Hardened Properties of High-Performance Printing Concrete." *Cement and Concrete Research* 42(3):558-566.

Li,Y., S. Zhou, J. Yin, and Y. Gao. 2009. "Effects of Fly Ash on the Fluidity of Cement Paste, Mortar, and Concrete." *International Workshop on Sustainable Development and Concrete Technology*. People's Republic of China (PRC): Central South University, pp 339-345.

Liesen, Richard, Peter Ellis, Alexander Zhivov, and Dale Herron. 2012. "Extremely Low Energy Design for Army Buildings: Barracks." *ASHRAE Transactions* 118:767-89.

Lim, S., R. A. Buswell, T. T. Le, S. A. Austin, A. G. F. Gibb, and A. Thorpe. 2012. "Development in Construction-Scale Additive Manufacturing Processes." *Automation in Construction* 21(1):262-268.

Lim, S., R. A. Buswell, T. T. Le, R. Wackrow, S. A. Austin, A. G. F. Gibb, and A. Thorpe. 2011. "Development of a Viable Concrete Printing Process." *ISARC 2011: The 28th International Symposium on Automation and Robotics in Construction*. Seoul, Korea: ISARC.

Mindess, S., J. F. Young, and D. Darwin. 2003. *Concrete*. 2nd ed. Upper Saddle Ridge, NJ: Prentice-Hall, Inc.

Mohamed, H. A. 2011. “Effect of Fly Ash and Silica Fume on Compressive Strength of Self-Compacting Concrete under Different Curing Conditions.” *Ain Shams Engineering Journal* 2:79-86.

Neville, A. M. 1996. *Properties of Concrete*. New York: Wiley & Sons, Inc.

Olivito, R. S., and F. A. Zuccarello. 2010. “An Experimental Study on the Tensile Strength of Steel Fiber Reinforced Concrete.” *Composites: Part B* 41(3):246-255, DOI 10.1016/j.compositesb2009.12.003.

Peled, A., M. Cyr, and S. Shah. 2000. “High Content of Fly Ash (Class F) in Extruded Cementitious Composites.” *ACI Materials Journal* 97(5):509-517, DOI 10.14359/9283.

Raharjo, D., A. Subakti, and Tavio. 2013. “Mixed Concrete Optimization Using Fly Ash, Silica Fume and Iron Slag on the SCC’s Compressive Strength.” *Procedia Engineering*, 54:827-839, DOI 10.1016/j.proeng.2013.03.076.

Richard, P., and M. Cheyrezy. 1995. “Composition of Reactive Powder Concretes.” *Cement and Concrete Research* 25(2):1501-1511.

Rushing, T. S., G. K. Al-Chaar, B. A. Eick, J. F. Burroughs, J. Shannon, and L. Barna. 2016. “Investigation of Concrete Mixtures for Additive Construction.” *Rapid Prototyping Journal*. Emerald Insight Publishing.

Shah, S. 1991. “Do Fibers Increase the Tensile Strength of Cement-Based Matrices?” *ACI Materials Journal* 88(6):595-602, DOI 10.14359/1195.

Smith, G. A., and S. W. Benham. 1931. “A Study of the Flow-Table and the Slump Test.” *ACI Materials Journal* 27(1):420-438.

Struble, L. 2006. “Hydraulic Cements – Physical Properties.” In *Significance of Tests and Properties of Concrete and Concrete-Making Materials*. J. Lamond and J. H. Pielert (eds.). STP 169D. West Conshohocken, PA: ASTM.

Taylor, P. C., S. H. Kosmatka, G. F. Voigt, and M. Brink (eds.). 2007. *Integrated Materials and Construction Practices for Concrete Pavement: A State-of-the-Practice Manual*. Publication No. HIF-07-004. Washington, DC: U.S. Department of Transportation (USDOT), Federal Highway Administration (FHWA).

Tregger, N. A., M. E. Pakula, and S. P. Shah. 2010. “Influence of Clays on the Rheology of Cement Pastes.” *Cement and Concrete Research* 40(3):384-391.

Tregger, N., T. Voigt, and S. Shah. 2007. “Improving the Slipform Process via Material Manipulation.” *Advances in Construction Materials 2007*. Springer-Verlag Berlin Heidelberg, pp 539-546.

Zhivov, Alexander, Richard J. Liesen, Stephan Richter, Reinhard Jank, David M. Underwood, Dieter Neth, Alfred Woody, Curt Bjork, and Scot Duncan. 2012. “Net Zero Building Cluster Energy Systems Analysis for U.S. Army Installations.” *ASHRAE Transactions* 118:751.

Acronyms and Abbreviations

Term	Definition
A&T	Agricultural and Technical
ACES	Automated Construction of Expeditionary Structures
ACH	Air Changes per Hour
ACI	American Concrete Institute
ACME	Additive Construction with Mobile Emplacement
AFCS	Army Facilities Component System
AFRICOM	U.S. Africa Command
ANSI	American National Standards Institute
ASAALT	Assistant Secretary of the Army for Acquisition, Logistics, and Technology
ASHRAE	American Society of Heating, Refrigerating, and Air-Conditioning Engineers
ASTM	American Society for Testing and Materials
BIM	Building Information Modeling
CBA	Capabilities Based Assessment
CBRN	Chemical, Biological, Radiological, and Nuclear
CE/MHE	Combat Engineer/Material Handling Equipment
CE/MHS	Combat Engineer and Material Handling Systems
CENTCOM	U.S. Central Command
CERL	Construction Engineering Research Laboratory
CMU	Concrete Masonry Unit
COCOM	Combatant Command
CONUS	Continental United States
CRADA	Cooperative Research and Development Agreement
CRREL	Cold Regions Research and Engineering Laboratory
CS&CSS	Combat Support and Combat Service Support
DGFS	Dry Goods Feed System
DMH	Domestic Hot Water
DOE	U.S. Department of Energy
DX	Direct Expansion
ECP	Entry Control Point
EFOB-L	ERDC-CERL Forward Operating Base Laboratory
ERDC	U.S. Army Engineer Research and Development Center
ERDC-CERL	Engineer Research and Development Center, Construction Engineering Research Laboratory
ERDC-CRREL	Engineer Research and Development Center, Cold Regions Research and Engineering Laboratory
ERS	Engineering Resilient Systems
EUI	Energy Use Intensity
FEMA	Federal Emergency Management Agency

Term	Definition
FHWA	Federal Highway Administration
FY	Fiscal Year
GCD	Game Changing Development
GSL	Geotechnical and Structures Laboratory
HVAC	Heating, Ventilating, and Air-Conditioning
IAA	Interagency Agreement
IC	Influence Coefficient
IECC	International Energy Conservation Code
IESNA	Illuminating Engineering Society of North America
ISARC	International Symposium on Automation and Robotics in Construction
JIIM	Joint, Interagency, Intergovernmental, and Multinational
KSC	Kennedy Space Center
MIPR	Military Interdepartmental Purchase Request
MSCoE	U.S. Army Maneuver Support Center of Excellence
MSFC	Marshall Space Flight Center
NASA	National Aeronautics and Space Administration
NORTHCOM	U.S. Northern Command
NREL	National Renewable Energy Laboratory
NSN	National Supply Number
OMB	Office of Management and Budget
PEO	Program Executive Officer
PLS	Palletized Load System
PRC	People's Republic of China
PTAC	Packaged Terminal Air Conditioner
SAR	SAME As Report
SF	Standard Form
SOUTHCOM	U.S. Southern Command
SRA	Shrinkage-Reducing Admixture
TR	Technical Report
TRADOC	U.S. Army Training and Doctrine Command
USACE	U.S. Army Corps of Engineers
USC	University of Southern California
USDOT	U.S. Department of Transportation

Appendix A: Project Management

A.1 NASA partnership and contributions

A.1.1 NASA partnership

NASA's MSFC has been investigating an additive construction technique known as "contour crafting" for over a decade for use in constructing infrastructure on planetary surfaces from in-situ resources. Because of this history, MSFC has a strong relationship, and a sub-contract, with the inventor of contour crafting, Dr. Behrokh Khoshnevis. It is this direct link that has enabled the U.S. Army Corps of Engineers (USACE) to investigate contour crafting additive construction technology for use in theater.

The partnership between USACE and NASA has enabled execution of two closely parallel projects within each organization: the ACES project and the Additive Construction with Mobile Emplacement (ACME) project, respectively. Figure A-1 shows the areas of shared interest between the two. The partnership is in the form of an Interagency Agreement (IAA), with procurement funding contributed to NASA from USACE via a Military Intergovernmental Purchase Request (MIPR). Complementary Full Time Equivalent labor and procurement funding for the ACME project comes from NASA's Space Technology Mission Directorate Game Changing Development (GCD) Program through the MSFC-led Advanced Manufacturing Technologies project. NASA's KSC co-leads the ACME project with MSFC.

Figure A-1. Shared NASA and USACE interests in advancing the additive construction technique.

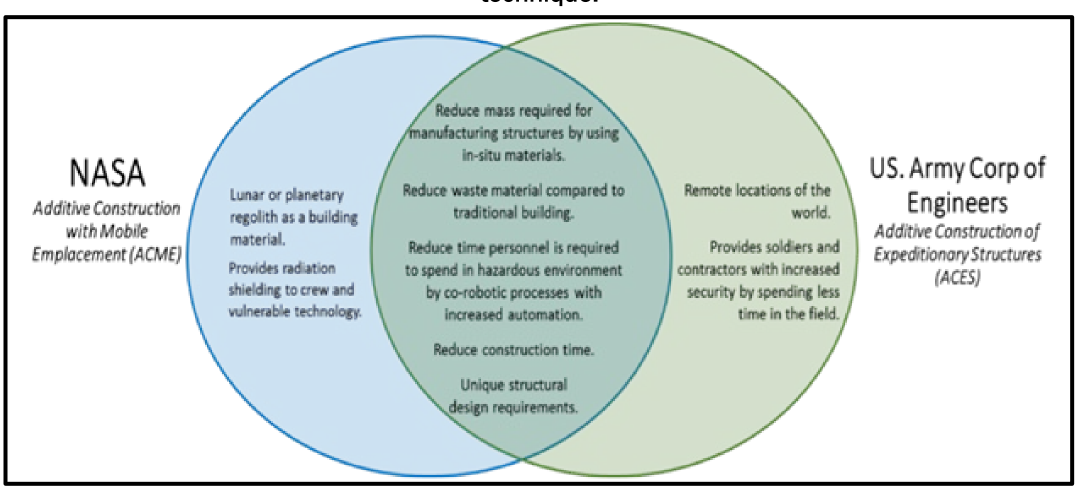

A.1.2 NASA contributions

ACME is focused on developing technolgies required to sort and process excavated materials into a feedstock with advanced planetary construction material properties, and to optimize these material compositions to be used with the additive construction process. ACME consists of subsystems that process, mix, and continuously feed a cement and planetary simulant mixture through a nozzle mounted on a mobility system (e.g., gantry). ACME has successfully demonstrated the ability to build straight and curved walls with martian regolith (soil) simulant, using a cement that can be produced from feedstock on the surface of Mars. The ACME system has received many upgrades this year, including the ability to continously deliver feedstock material to the nozzle. ACME has an advanced nozzle from Contour Crafting Corporation that, when combined with the continous feedstock delivery system and improved software, can pause operations to build windows and doors. USACE is integrating many of ACME's techniques, hardware, and expertise directly into ACES to demonstrate the ability to construct structures critical to Army operations such as barracks, Hesco barriers, and guard shacks.

A.1.2.1 Hardware - Accumulator

Figure A-2. Accumulator.

One of the desired capabilities of 3D printing is the ability to shut off the flow of material at will. The accumulator provides that capability. An accumulator is a device that allows pressure to build as needed while flow is stopped (accommodating a continuous flow of material from a pump), then releases the pressure slowly when flow continues. The accumulator provided to USACE for the ACES 2nd generation system, conceptually shown in Figure A-2, was built at MSFC from a modified design from Dr. Khoshnevis.

A.1.2.2 Hardware – Liquid delivery system

To provide sufficient material to the mixer to build a B-Hut within 24 clock hours, feedstock delivery must be predictable and high-volume. To accommodate this requirement, MSFC engineers developed and built a system to assist in dispensing liquid goods, including water and concrete admixtures (Figure A-3). This system attaches to a water hose and uses a refillable water tank to meter out a sufficient volume of water for each batch of concrete. The dispensing capability of the water tank is controlled by an electronic display. The operator needs only to program how much water is to be dispensed, and the control system and pump will meter out the appropriate amount. Admixtures are contained in tanks behind the water tank. These admixtures are measured by hand, by volume, using provided measuring bottles.

Figure A-3. Liquid delivery system.

A.1.2.3 Hardware – Dry goods feed system

The KSC ACME team, with their strong expertise in granular mechanics, designed and is currently building a delivery system for the dry goods. These dry goods include up to seven materials: ⅜ inch pea gravel, coarse sand, fine sand, Portland cement, and other concrete additives. The goods are kept in bins, weighed via load cells in a weigh bin, and delivered by constituent-specific motor driven auger feed systems. Figure A-4 illustrates the concept of the Dry Goods Feed System (DGFS).

Figure A-4. DGFS computer aided design model.

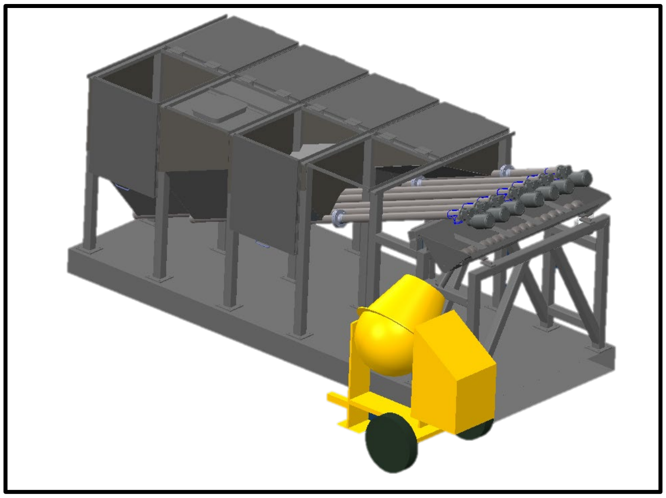

The large quantities of dry materials required to build a B-Hut must be efficiently stored in weather resistant containers and then accurately dispensed into a concrete mixing device for subsequent delivery to the ACES additive construction system. The DGFS consists of a robust painted steel weldment and associated mechanisms for feeding the materials. Each DGFS can hold the total concrete materials that are required to build a B-Hut, and yet it can be transported (when empty) on a C-130 transport aircraft with the rest of the system since it weighs less than 10,000 pounds. The DGFS dimensions are 8x8x20 ft (WxHxL). It can be lifted and deployed very quickly due to its fully integrated design. The control system is user-friendly with a high level of automation so that Soldiers in the field can easily operate it. The key to having a good additive construction process is to have the correct concrete slurry before pumping to the print nozzle. The DGFS achieves this, in combination with the other elements in the ACME/ACES system.

A.1.2.4 Expertise – Critical material properties for additive construction

To use additive construction technology, one must have a mixture that is sufficiently liquid to pump, but sufficiently solid to build on. Additionally, the material must be strong enough to bear the weight of a roof within a small amount of time after printing. This can be a difficult problem to tackle. Over the course of Fiscal Year 2016 (FY16), both NASA and USACE have actively pursued compositions of materials to make use of additive construction possible. Both organizations have shared lessons learned with regard to material development (Table A-1).

Table A-1. Example issues and lessons learned from the ACES and ACME teams.

Issue	Lesson Learned	Go-Forward Plan
Accumulator for ACES 2 jammed with ⅜-in. pea gravel	Increasing aggregate size increases pressure, aggregate settles when under significant pressure.	Redesign accumulator to accommodate increased pressure; adjust accumulator tube diameter or mixture to decrease the amount of settling by aggregate.
Air pockets in concrete flow	Pump speed must be high enough to accommodate gravity drop from vertical hose length above nozzle assembly, or vertical hose length must be reduced.	Modify vertical hose length and adjust pump speed to eliminate interruptions in the concrete flow.
Inconsistent width of bead	There must be enough concrete in the pump to maintain pressure on the pump mechanism.	Define a “minimum pump volume” level.
Making the additive construction process more reproducible between batches	Material properties must be within a certain range of viscosity to fulfill pumpability and stiffness (lack of slump) constraints for use in additive construction.	Measure viscosity of materials before printing and adjust mixture as necessary to keep the viscosity within a certain range.

A.1.3 NASA and terrestrial benefits

The vision of ACME is to enable science and human exploration by using in-situ resources that feed additive construction techniques to efficiently build needed infrastructure. It is estimated that between 60 and 90% of mass savings can be realized by reducing the amount of material launched from earth by using in-situ materials and the automated additive construction technique. Automated additive construction can be used to build both terrestrial and extraterrestrial structures while reducing time and cost required to transport materials, reducing waste compared to traditional construction techniques, and reducing the exposure of personnel to hazardous environments through increased automation. The success of the ACME and ACES projects has caught the eye of the construction industry with a proposed partnership from an industry leader, with high potential for future technology transfer.

A.2 Major milestones

FY15 and FY16 had two major milestones:

1. To build a full-scale ~ 6x6-ft Entry Control Point (ECP) guard shelter inside the high bay area at the ERDC-CERL by April 2016
2. To build a full-scale 16x32-ft B-Hut at the ERDC Forward Operating Base Laboratory at ERDC-CERL by August 2016.

A.3 Technology transfer

The proponents for this project include the MSCoE and the Product Manager for Combat Engineer/Material Handling Equipment (PdM CE/MHE), under the Program Executive Office for Combat Support and Combat Service Support (CS&CSS). The program team has worked with MSCoE and the PdM CE/MHE during the project to ensure that the research satisfies Army and joint requirements. As part of the formal vetting process, the program team agreed to maintain continuous interaction with the MSCoE proponents. To satisfy this, both MSCoE and the PdM were contacted at least quarterly and briefed at least annually on progress of the research program. In addition, both organizations were invited to ERDC-CERL to view ACES 1 and ACES 2 to witness significant milestones (such as scaled experiments), and to witness a proof-of-concept demonstration of full-size shelter 3D printing. PdM CE/MHE has agreed to provide flatrack specifications, a mocked-up PLS platform, and one or two PLS vehicles for a proof-of-concept demonstration. Pending successful completion of the proof-of-concept prototype, ERDC will seek a Technology Transition Agreement with Program Executive Officer (PEO) CS&CSS.

A.3.1.1 Publications

The following technical reports, journal papers, and media were completed or are planned. Industry publications such as Engineering News Record will be targeted with news releases following major milestones, such as successful scale models, gantry/arm down-select, and successful full-scale prototypes.

- FY15
    - Video Animation - Automated Construction of Expeditionary Structures Concept of Operations
- FY16
    - Technical Report - Thermal and Mechanical Properties of Additively Constructed Wall Sections (delayed to FY 16 due to late delivery of concrete pump)
    - Technical Report & Journal Paper - Flow Characteristics and material properties of concrete mixtures for additive construction
    - Journal Paper (Architecture) - Design and structural analysis of medium-sized structures using layered concrete construction
    - Journal paper - Cold Weather behavior of concrete mixtures used for layered construction

  - Journal paper - Resistance of novel concrete structure shapes created using layered construction.
- FY17
  - Final Technical Report - Automated Construction of Expeditionary Structures
  - Journal Paper - Comparison of gantry vs. boom-mounted robotic actuator in layered concrete construction.

A.3.1.2 Patents

Some of the technologies that will be used and improved in this project are already patented, chiefly by USC. Several new patentable ideas are anticipated, especially in the areas of ground preparation, control systems, concrete mixtures, wall configuration, lintel design, and roofing. Design notebooks will be maintained for patent purposes and patent applications submitted where appropriate.

A.3.1.3 Potential post-FY17 follow-on efforts

A successful proof-of-concept is expected to lead to further research and transition opportunities. Most important, perhaps, is to obtain PEO CS&CSS participation in incorporating the technology into the acquisition process as an Army system that can be mounted on Army vehicles (such as the PLS). The program will pursue opportunities with Combatant Commands (COCOMs) for demonstrations, especially U.S. Southern Command (SOUTHCOM), U.S. Africa Command (AFRICOM), U.S. Central Command (CENTCOM) and the U.S. Northern Command (NORTHCOM) (for cold regions). The program has also pursued opportunities with the Marine Corps for printing of potential wall thicknesses and designs. Follow-on research includes use of indigenous materials such as adobe or engineered soils; and use of naturally occurring materials such as chitin, that could be tuned for engineered lifetimes (i.e., to be biodegradable). The program will seek industry involvement to promote dual-use application in the commercial construction market.

REPORT DOCUMENTATION PAGE

Form Approved
OMB No. 0704-0188

1. REPORT DATE (DD-MM-YYYY)	2. REPORT TYPE	3. DATES COVERED (From - To)
02/01/2021	Final Report	

4. TITLE AND SUBTITLE
Automated Construction of Expeditionary Structures (ACES): Energy Modeling

5a. CONTRACT NUMBER

5b. GRANT NUMBER

5c. PROGRAM ELEMENT

6. AUTHOR(S)
Brandy N. Diggs, Richard J. Liesen, Sameer Hamoush, Ahmed C. Megri, and Michael P. Case

5d. PROJECT NUMBER
622784AT41; 622784T45; 633728002

5e. TASK NUMBER

5f. WORK UNIT NUMBER

7. PERFORMING ORGANIZATION NAME(S) AND ADDRESS(ES)
U.S. Army Engineer Research and Development Center (ERDC)
Construction Engineering Research Laboratory (CERL)
PO Box 9005,
Champaign, IL 61826-9005

8. PERFORMING ORGANIZATION REPORT NUMBER
ERDC/CERL TR-21-6

9. SPONSORING / MONITORING AGENCY NAME(S) AND ADDRESS(ES)
Assistant Secretary of the Army for Acquisition, Logistics, and Technology (ASAALT)
103 Army Pentagon
Washington, DC 20314-1000

10. SPONSOR/MONITOR'S ACRONYM(S)
CEERD-CZT

11. SPONSOR/MONITOR'S REPORT NUMBER(S)

12. DISTRIBUTION / AVAILABILITY STATEMENT
Approved for public release; distribution is unlimited.

13. SUPPLEMENTARY NOTES

14. ABSTRACT
The need to conduct complex operations over time results in U.S. forces remaining in deployed locations for long periods. In such cases, more sustainable facilities are required to better accommodate and protect forward deployed forces. Current efforts to develop safer, more sustainable operating facilities for contingency bases involve construction activities that redesign the types and characteristics of the structures constructed, reduce the resources required to build, and reduce resources needed to operate and maintain the completed facilities. The Automated Construction of Expeditionary Structures (ACES) project was undertaken to develop the capability to "print" custom-designed expeditionary structures on demand, in the field, using locally available materials with the minimum number of personnel. This work investigated large-scale automated "additive construction" (i.e., 3D printing with concrete) for construction applications. This document, which documents ACES energy and modeling, is one of four technical reports, each of which details a major area of the ACES research project, its research processes, and associated results, including: System Requirements, Construction, and Performance; Energy and Modeling; Materials and Testing; Architectural and Structural Analysis.

15. SUBJECT TERMS
United States--Armed Forces--Military construction operations, Construction--Automation, Military bases, Three-dimensional printing, Concrete construction, Energy consumption

16. SECURITY CLASSIFICATION OF:			17. LIMITATION OF ABSTRACT	18. NUMBER OF PAGES	19a. NAME OF RESPONSIBLE PERSON
a. REPORT	b. ABSTRACT	c. THIS PAGE			19b. TELEPHONE NUMBER (include area code)
Unclassified	Unclassified	Unclassified	SAR	75	